Universiteit
Leiden
The Netherlands

Synthetic peptides as tools in chemical immunology

Doelman, W.

Citation
Doelman, W. (2023, February 9). *Synthetic peptides as tools in chemical immunology*. Retrieved from https://hdl.handle.net/1887/3563057

Version:	Publisher's Version
License:	Licence agreement concerning inclusion of doctoral thesis in the Institutional Repository of the University of Leiden
Downloaded from:	https://hdl.handle.net/1887/3563057

Note: To cite this publication please use the final published version (if applicable).

7

Summary and future prospects

R.C. Reijnen contributed to the thioflavin T assays described in this chapter.

S. Wijngaarden contributed to the protein synthesis described in this chapter.

This thesis has described novel synthetic methods to produce a variety of (glyco)peptides and their application in the study of various immunological processes. The first part of the thesis describes novel insights into the pathogenesis of multiple sclerosis, in the form of new findings in the areas of lectin-driven immunotolerance and a biochemical comparison between human and animal model antigen.[1,2] The next part describes novel multivalently glycosylated peptides, that can be used to study lectin binding and lectin mediated antigen uptake.[3,4] The final part of the thesis describes a novel method to produce *trans*-cyclooctene protected peptides, an exciting new category of molecular tools within chemical biology that have recently been developed.[5]

Chapter 2 describes the synthesis of a series of N-glycosylated Fmoc-asparagine building blocks for solid phase peptide synthesis (SPPS). Four different glycan structures were synthesized: GlcNAc, LacNAc (Galβ1-4GlcNAc), Fucα1-3GlcNAc and Lewis X (Galβ1-4(Fucα1-3)GlcNAc, Le^X). The building blocks were constructed from the protected glycosyl azides and coupled to the sidechain of asparagine using a one-pot, two step procedure involving Staudinger reduction of the azide followed by regioselective ring-opening of Fmoc-aspartic anhydride. Using standard Fmoc-SPPS conditions, these building blocks were incorporated into the immunodominant peptide of myelin oligodendrocyte glycoprotein (MOG), MOG_{31-55}, at the site of native N-glycosylation (Asn_{31}). Using an ELISA based assay, binding of the Le^X decorated neoglycopeptide to DC-SIGN was proven. Furthermore, a Le^X dependent effect on cytokine secretion, specifically a decrease of IL12p70 secretion, was found when moDCs were treated with peptides in presence of LPS. The effect of glycosylation on the citrullination driven aggregation of MOG_{31-55} was also investigated. Here a glycosylation-dependent decrease in aggregation propensity was found.

Synthesis and immunological evaluation of neoglycopeptides bearing these *N*-glycosylated asparagine residues could lead to a better understanding of glycosylation mediated cytokine secretion. Since these building blocks are far easier to obtain in synthetically useful quantities then native, Le^X decorated N-glycosylated asparagine, while still containing a native glycosidic linkage to the peptide, they could be highly useful in situations were side effects resulting from non-native linkages are to be avoided. Furthermore, the interplay of glycosylation and citrullination on the aggregation of MOG_{31-55} remains an interesting topic.

With the GlcNAc decorated MOG_{31-55} peptides easily available, native N-glycan structures could be introduced by the use of engineered *endo*-β-N-acetylglucosaminidase (ENGase) enzymes.[6] ENGase enzymes are naturally able to cleave the glycosidic bond between the two GlcNAc residues in the chitobiose core of an *N*-glycan, but directed mutagenesis produced enzymes that can instead ligate a GlcNAc decorated asparagine together with a glycan containing a reducing end GlcNAc, provided this GlcNAc is provided as the oxazoline.[7] Using this approach, peptides bearing native *N*-glycans, for instance the high-mannose type[8] or sialylated complex type,[9] can be synthesized.[10] Using these methods, different forms of natively glycosylated MOG_{31-55} could be produced, and the effects of native glycosylation on citrulline driven aggregation evaluated.

Chapter 3 reports the evaluation of a series of citrullinated peptides derived from the myelin protein myelin oligodendrocyte glycoprotein (MOG). Previous work has found that the murine sequence of the immunodominant peptide MOG_{35-55} displayed amyloid-like aggregation behavior after citrullination.[2] The MOG protein, and particularly the immunodominant region, have a high degree of similarity between species, and the only amino acid substitution between the murine and human sequence is a Ser-to-Pro substitution on position 42. Experiments described in chapter 3 indicate that this single substitution fully inhibits the aggregation. Some further chemical mutagenesis experiments were carried out, replacing

Ser_{42} with various serine isosteres, indicating serine to be crucial for the citrullination driven aggregation.

An additional surprising difference between the marmoset Ser_{42} containing citrullinated MOG_{35-55} peptides and the human Pro_{42} containing variants came from an antigen cross-presentation assay. Using B- and T-cells from marmosets previously immunized with $hMOG_{35-55}$,[11] it was found that one of the non-aggregating human MOG_{35-55} variants was better able to activate T-cells than the corresponding aggregating marmoset variant. Specifically, the marmoset peptide $mMOG_{35-55}Cit_{46,52}$, a strongly aggregating peptide, did not produce any T-cell response, while the non-aggregating $hMOG_{35-55}Cit_{46,52}$ did. Given the complexity of the underlying immunology, determining the precise cause of this discrepancy can be multi-factorial. In this chapter, two major hypotheses for the difference in T-cell activation are proposed and evaluated.

The first hypothesis involved the presentation of the antigen to the T-cell. In order for an antigen to elicit a T-cell response, an epitope, a peptide usually 8 or 9 residues in length, has to be loaded into a Major Histocompatibility Complex (MHC), and this epitope-MHC complex has to be recognized by a T-cell receptor (TCR). The precise structure of this epitope-MHC complex, especially the exact binding mode of the epitope, is often critical for TCR recognition. The critical question here is whether the citrullination pattern leading to aggregation affects the position of the amino acid sidechains in the MHC-complex. While the structure of the MHC-peptide complex has not been determined experimentally, computational methods can be used to study these interactions *in silico* by docking the peptide into the MHC crystal structure. This method will be applied to evaluate whether differences in presentation of the epitope are to be expected to play a role in the observed differences in T-cell activation.

The second hypothesis was that the amyloid-like aggregation behavior prevents the proteolytic liberation of the minimal epitope from the aggregated longer MOG-peptide fragments, leading to reduced antigen presentation. The epitope, to be loaded into an MHC, needs to be liberated from the full 21-mer peptide incubated with the cell. To produce this epitope, which is only 9 residues in length, partial degradation of the longer peptide is required. This process is called antigen processing and is quite difficult to study, due to the amount of enzymes and cell-compartments it involves.[12] Still, differences in degradation of the peptide, caused by either the introduction of the citrulline residues in the peptide sequence, or by the difference between the Ser-containing marmoset peptide compared to the Pro-containing human one, could lead to differences in peptide degradation. This hypothesis was approached from two directions. First, it was investigated whether smaller peptides derived from $mMOG_{35-55}$-$Cit_{46,52}$ retained the ability to aggregate, which could prevent loading of this peptide into MHC complexes (thereby preventing T-cell activation). To answer this question, the citrullinated forms of the MHC binding epitope (MOG_{40-48}),[13] as well as C- and N-terminally extended versions of this peptides, were evaluated for their aggregation propensity. Alternatively, the liberation of the specific epitope could be impeded by the inability of a specific enzyme to perform its proteolytic function, or by a specific enzyme

destructively processing the key epitope. Previously, Cathapsin G (CatG) degradation was implicated as major factor in the degradation of MOG_{35-55} antigens[14,15] and has also been shown to be critical in the degradation of a different myelin antigen (myelin basic protein, MBP) by B-cells.[16] Therefore, the degradation of the different MOG_{35-55} peptides by this enzyme was investigated.

Docking of MOG_{40-48} peptides into HLA-E

While the antigenicity of citrullinated $hMOG_{35-55}$ has never been studied in the marmoset system, previous work in mice[17] showed that citrullination of $mMOG_{35-55}$-Cit_{46} strongly diminished the immune response observed from T-cells of $mMOG_{35-55}$ immunized animals, similar to absence of T-cell responses against $mMOG_{35-55}$-$Cit_{46,52}$ seen in Chapter 3. The presentation of $hMOG_{35-55}$ to T-cells via EBV infected marmoset B-cells is considered to take place via presentation on the non-classical MHC class I receptor Caja-E.[13] Since no crystal structures of the peptide-MHC complexes are available, it is unknown whether the presentation of the human and marmoset MOG_{40-48} in the relevant MHC displays the same TCR (T-cell receptor) contact residues.

To evaluate binding difference inside the Caja-E complex, an *in silico* docking approach was used to predict the binding of the different MOG_{40-48} epitopes to this MHC. This approach was previously used to study the effect of citrullination on a key T-cell epitope of a protein involved in rheumatoid arthritis, where a large perturbation of a residue was predicted for the citrullinated peptide, potentially explaining the lack of T-cell response against this peptide.[18] If docking of the different MOG_{40-48} epitopes shows a similar perturbation only for $mMOG_{40-48}$-Cit_{46}, this could help explain the observed effect. While no crystal structures of Caja-E have been reported, the amino acid sequence shows extremely high similarity to human HLA-E, for which multiple structures are available. Careful examination of the polymorphisms present between Caja-E and HLA-E showed that no amino acid polymorphisms were present in the binding cleft (Figure S1). Therefore, the available HLA-E structures were considered decent models for the study.

For the purpose of the docking study, it was assumed that citrullination of Arg_{46} and Arg_{52} would not lead to different processing of the peptide, and therefore would produce a different 9-mer epitope from MOG_{40-48}. The following four different forms of MOG_{40-48} expected to be produced by the B-cell during processing were docked: $hMOG_{40-48}$, $mMOG_{40-48}$, $hMOG_{40-48}$-Cit_{46} and $mMOG_{40-48}$-Cit_{46}. When comparing the poses found when docking either the human or marmoset form of the epitope (Figure 1A), the N-terminal part of the peptides seems to overlay quite well, even on the position of the Pro/Ser polymorphism. The rest of the sequence shows less overlap, with the central phenylalanine showing a large shift in location in the binding cleft. The C-terminal valine again overlaps well between the two peptides, indicating correct docking of the peptide's carboxylic acid.

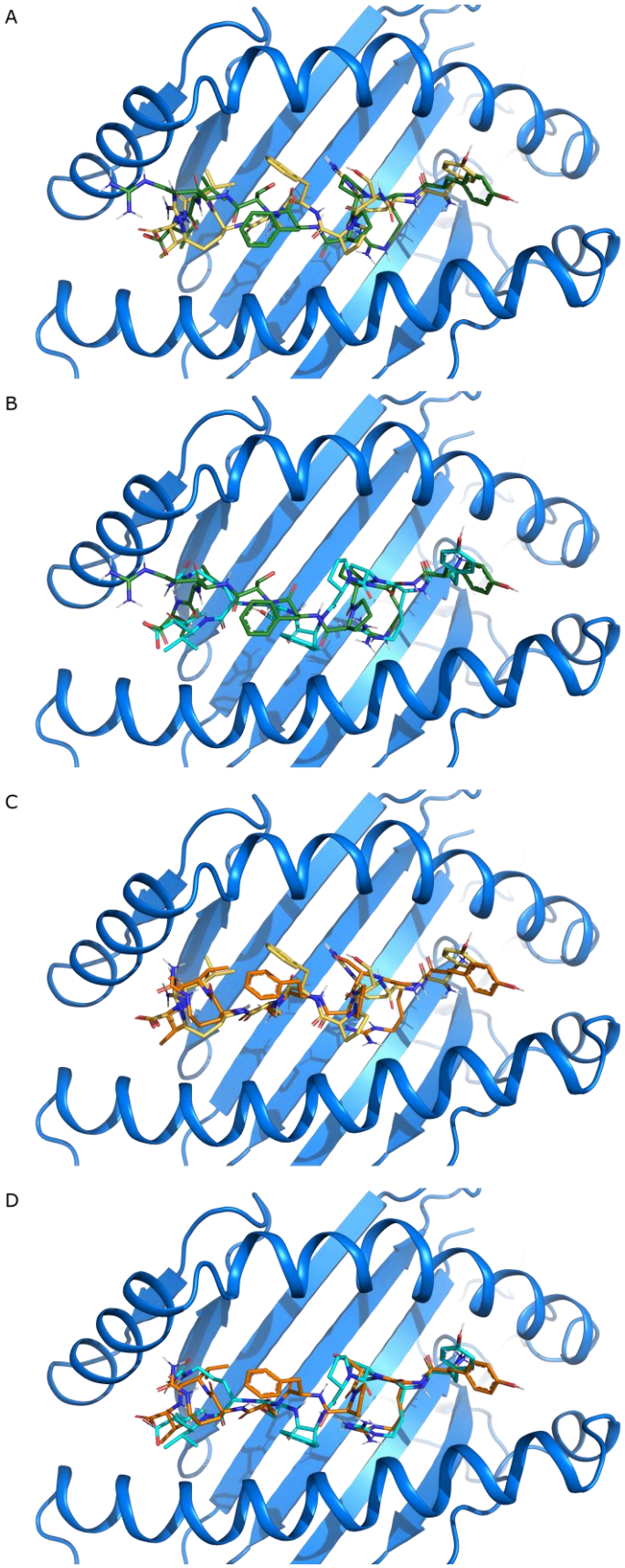

Figure 1. Resulting poses after docking the four different MOG_{40-48} peptides into HLA-E. The following colors were used to denote the different peptides: $hMOG_{40-48}$ (green), $mMOG_{40-48}$ (yellow), $hMOG_{40-48}$-Cit_{46} (cyan), $mMOG_{40-48}$-Cit_{46} (orange) A) $hMOG_{40-48}$ compared with $mMOG_{40-48}$ B) $hMOG_{40-48}$ and $hMOG_{40-48}$-Cit_{46} C) $mMOG_{40-48}$ and

mMOG$_{40-48}$-Cit$_{46}$ D) hMOG$_{40-48}$-Cit$_{46}$ and mMOG$_{40-48}$-Cit$_{46}$. These docking studies were performed by A.P.A. Janssen (Leiden university).

When comparing the human wildtype and citrullinated form (Figure 1B), good overlap was again observed for the three N-terminal residues. On the C-terminal side, the backbone of the citrullinated residue is twisted, resulting in the citrulline pointing more inward into the cleft, making the penultimate valine solvent exposed. The docked poses found for wildtype mMOG$_{40-48}$ and its citrullinated counterpart (Figure 1C) are highly similar, with the backbone closely overlapping over its entire length.

Figure 1D shows the overlay of the docking poses found for the human and marmoset citrullinated peptides. Based on the results of the T-cell presentation assay (Chapter 3) this is where the largest differences are expected. However, as expected from the high degree of overlap between both wildtype peptides and their citrullinated counterparts, the same pattern is found in the direct comparison, with the N-terminus overlapping well and the C-terminus showing a conformational difference. Taken together, these findings do not give a strong basis to explain the differences found in the T-cell activation assays. This suggests that differences in antigen processing is the major factor in the changes in antigen presentation. This could be due to the altered solubility/aggregation of the processed peptides, for instance by aggregation sequestering the epitope inside insoluble aggregates. Altered processing, either due to partially processed peptides forming aggregates, or due to differential proteolysis of peptides due to citrullination could also be relevant. These ideas will be explored in the rest of this chapter.

Aggregation of truncated peptides

Having shown that the human-variant of MOG$_{35-55}$ did not aggregate upon citrullination like the marmoset citrullinated peptide, it was next assessed whether truncated versions of the marmoset peptide retained their ability to aggregate. Since APCs would likely (partially) degrade internalized peptide, the aggregation behavior of peptide fragments could be just as important as that of the parent peptides, in an immunological setting.

First, the minimal MHC class I-restricted epitope peptide, MOG$_{40-48}$, was evaluated. Since this peptide contains two of the key arginine residues within the sequence (Arg$_{41}$ and Arg$_{46}$), a question was whether the citrullinated variants of this short 9-mer peptide could induce amyloid-like aggregation similar to that seen with the parent peptide. The three possible citrullinated variants of the mMOG$_{40-48}$ peptide, mMOG$_{40-48}$-Cit$_{41}$, mMOG$_{40-48}$-Cit$_{46}$ and mMOG$_{40-48}$-Cit$_{41,46}$ were synthesized on chlorotrityl resin, to obtain the free C-terminal carboxylic acid (Table 1). These were then tested in the same ThT assay as described in Chapter 3. None of these peptides showed any increase in ThT fluorescence over the 16 hour time

period, indicating none of the three the citrullinated peptides showed amyloidogenic properties as determined by ThT (Figure 2).

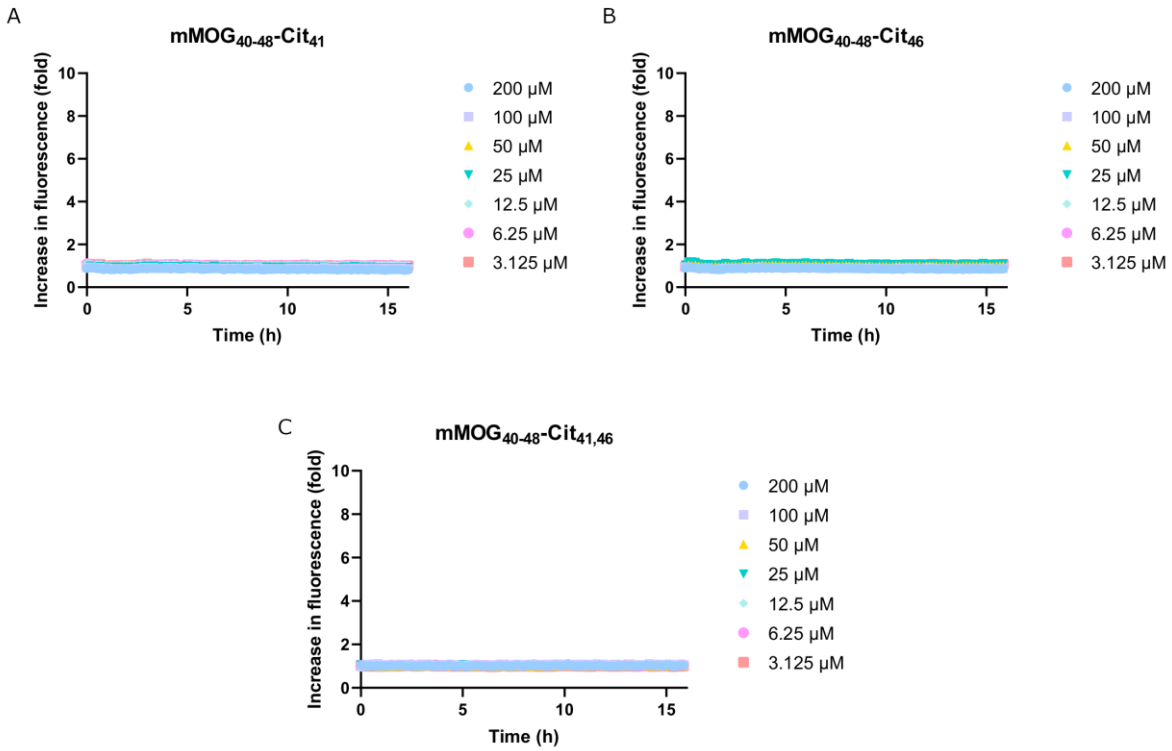

Figure 2. ThT aggregation assays showing the aggregation properties of citrullinated mMOG$_{40-48}$ peptides. A) mMOG$_{40-48}$-Cit$_{41}$. B) mMOG$_{40-48}$-Cit46. C) mMOG$_{40-48}$-Cit$_{41,46}$

Since the 9-mer T-cell epitopes did not show any amyloid-like aggregation, a key question was what the shortest aggregating sequence would be. Additionally, the aggregation kinetics of any shorter aggregating sequences could be important during antigen processing; rapid amyloidogenesis of a partially processed antigen could obstruct further degradation and MHC loading. To investigate this line of reasoning, a series of peptides was synthesized, each stepwise elongated by one residue on both the C- and N-terminus. All of these peptides were synthesized as the free carboxylic acid, to simulate degradation products that could be produced when mMOG$_{35-55}$-Cit$_{46,52}$ is degraded intracellularly. An overview of these synthetic, stepwise elongated peptides is given in Table 1.

Table 1. Overview of all novel peptides synthesized in this Chapter. Arginine residues that were replaced with citrulline are highlighted in boldface. All yields are after RP-HPLC and based on the manufacture specified resin loading.

Name	Sequence	Yield (%)
mMOG$_{40-48}$-Cit$_{41}$	Y**R**SPFSRVV	31
mMOG$_{40-48}$-Cit$_{46}$	YRSPFS**R**VV	29
mMOG$_{40-48}$-Cit$_{41,46}$	Y**R**SPFS**R**VV	33
mMOG$_{39-49}$-Cit$_{46}$	WYRSPFS**R**VVH	17
mMOG$_{38-50}$-Cit$_{46}$	GWYRSPFS**R**VVHL	27
mMOG$_{37-51}$-Cit$_{46}$	VGWYRSPFS**R**VVHLY	27
mMOG$_{36-52}$-Cit$_{46}$	EVGWYRSPFS**R**VVHLYR	13
mMOG$_{36-52}$-Cit$_{46,52}$	EVGWYRSPFS**R**VVHLY**R**	27
mMOG$_{35-53}$-Cit$_{46,52}$	MEVGWYRSPFS**R**VVHLY**R**N	27

The first three extensions, mMOG$_{39-49}$-Cit$_{46}$ (Figure 3A), mMOG$_{38-50}$-Cit$_{46}$ (Figure 3B) and mMOG$_{37-51}$-Cit$_{46}$ (Figure 3C) showed no increase in ThT fluorescence. However, the next extension, mMOG$_{36-52}$-Cit$_{46}$, showed a minor increase in ThT fluorescence over time (Figure 3D). The peptide containing 2 citrulline residues, mMOG$_{35-55}$-Cit$_{46,52}$, yielded a more pronounced aggregation (Figure 3E), that was further compounded when the N- and C-termini were extended by an additional amino acid (mMOG$_{35-53}$-Cit$_{46,52}$; Figure 3F). This compound showed aggregation behavior in line with the parent peptide mMOG$_{35-55}$-Cit$_{46,52}$ (Chapter 3, Figure 2F). The only caveat was that the lower concentrations did not show any increase in ThT fluorescence, in stark contrast to the full-length peptide.

These results imply it is primarily the non-processed peptide that is involved in amyloid-like aggregation and aggregation of a citrullinated, partially processed peptide is unlikely to be a key factor in the observed lack of T-cell activation. The key question that remains is whether the aggregation of the parent peptide by itself inhibits processing at the earliest point in the process.

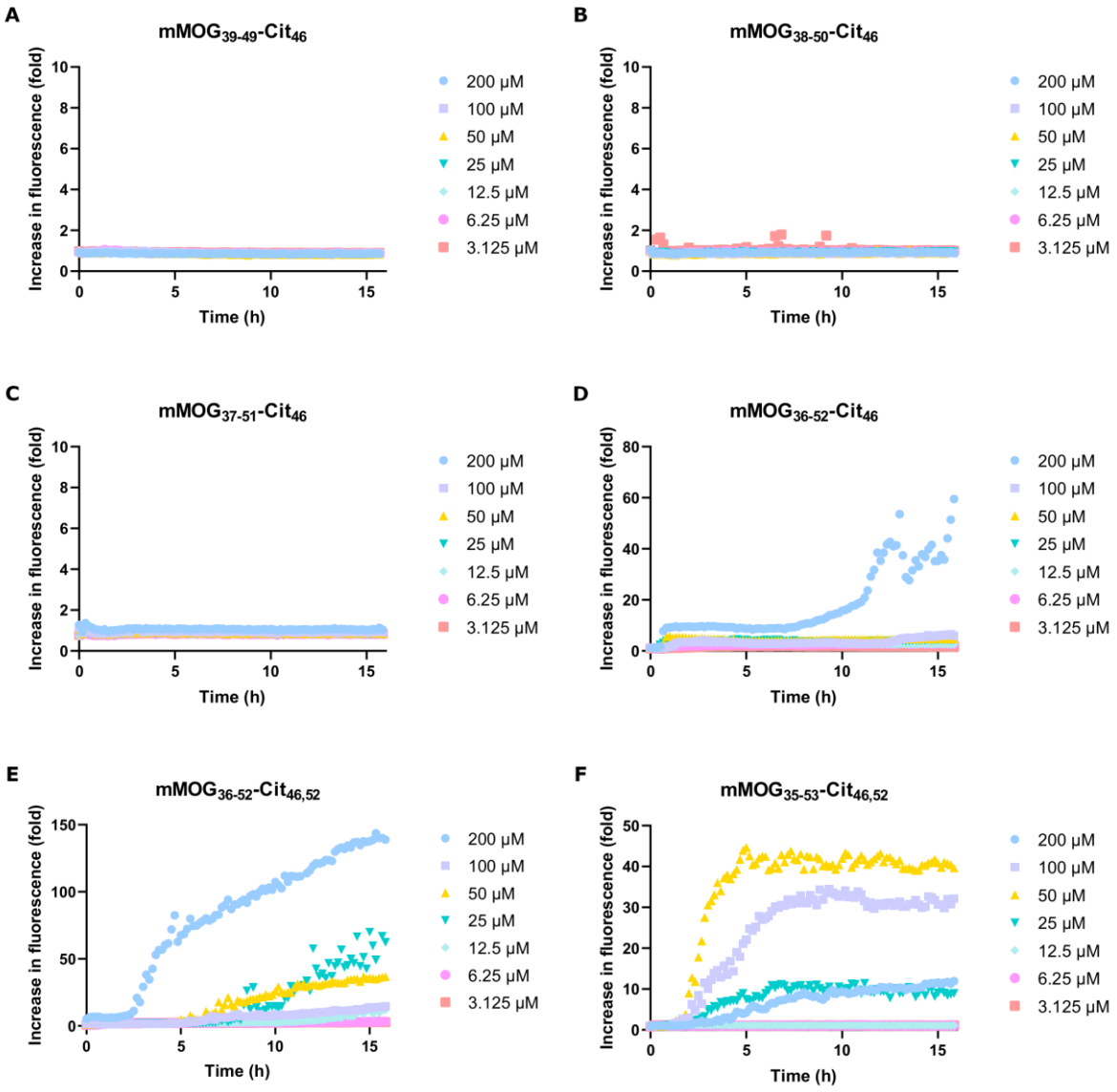

Figure 3. ThT aggregation assays of the stepwise elongated core epitope peptides. All sequences were based on the marmoset peptide sequence and in each step the peptide was elongated with one amino acid on both N- and C-terminus. A) $mMOG_{39-49}$-Cit_{46}. B) $mMOG_{38-50}$-Cit_{46}. C) $mMOG_{37-51}$-Cit_{46}. D) $mMOG_{36-52}$-Cit_{52}. E) $mMOG_{36-52}$-$Cit_{46,52}$. F) mMOG35-53-$Cit_{46,52}$

Alternative degradation by an endolysosomal protease

Cathepsin G (CatG) has been implicated as a crucial protease in the processing of MOG_{35-55}. Previous work suggested that this serine protease would destructively process the critical MOG_{40-48} epitope, unless Arg_{46} was citrullinated.[14,15] Destructive processing of amyloid autoantigen in B cells has also been implicated as an important mechanism for tolerance to myelin basic protein.[16] To more clearly understand the effect of citrullination on the degradation of the human and marmoset forms of MOG_{35-55}, both the non-citrullinated and $Cit_{46,52}$ forms of marmoset and human MOG_{35-55} were incubated with purified hCatG for 24 hours at 37°C and pH 5. At timepoints 0, 1, 2, 4 and 24 hours a sample was taken and measured

by LC-MS. The disappearance of the starting peptides was quantified and the data was plotted in Figure 4A.

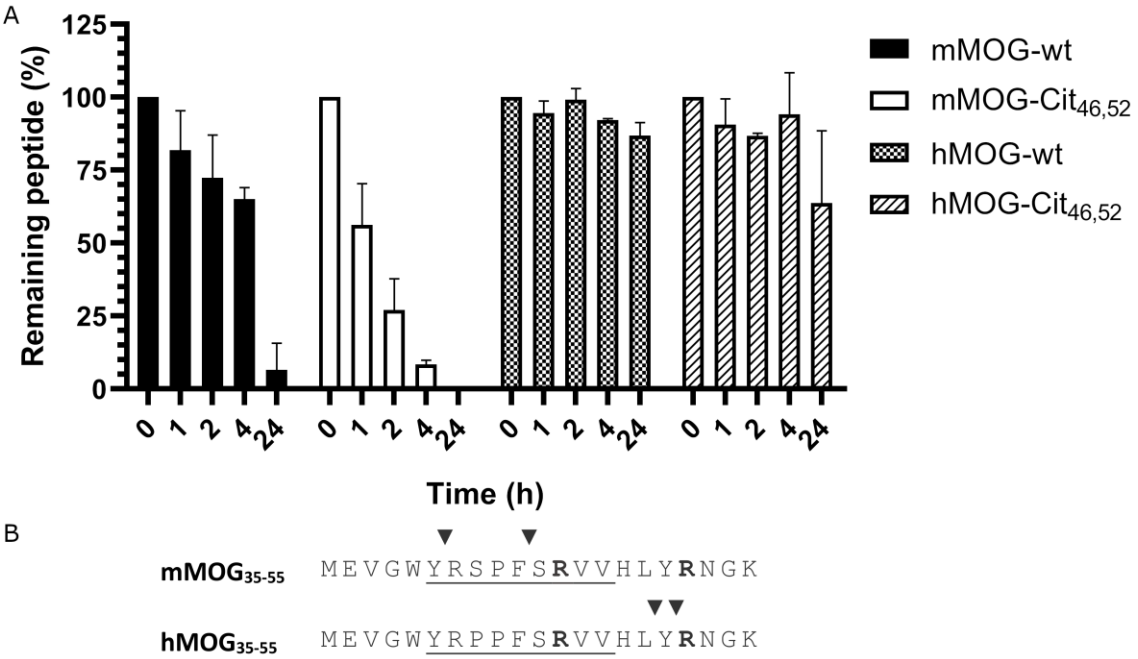

Figure 4. A) Degradation of peptides with human Cathepsin G at 37°C and pH 5. Peptides (10 µM) were incubated with hCatG (250 ng/mL) and samples were taken out at the stated time points and enzymatic activity was stopped by dilution of a 45:45:10 mixture of H_2O/MeCN/TFA. The samples were analyzed using LC-MS and amount of degradation determined by comparison of peak area against an internal standard. The graph shows the average of two independent experiments for each peptide. B) Mass spectrometry analysis was used to determine the cleavage sites of hCatG by analyzing the mass-spectra of the fragments formed after degradation. Arrows indicated detected cleavage sites. The immunodominant epitope MOG_{40-48} is underlined and the citrullinated arginine residues highlighted in bold.

The marmoset peptide $mMOG_{35-55}$ showed clear degradation over time, with the peptide being almost fully degraded after 24 hours. In contrast to what was seen by Jagessar *et al.*[14], the peptide containing citrulline on position 46 (as well as on position 52) was degraded by hCatG at an increased rate, with almost all peptide cleaved after only 4 hours. Earlier work on the sequence preference of hCatG showed that an acidic, negatively charged residue is preferred on the P2' position,[19] which could explain why neutral citrulline in P2' results in a higher rate of hydrolysis compared to positively charged arginine.

For the human peptides, degradation occurred sluggishly for either sequence. This might be explained by examining the peptide fragments formed by hCatG for the different peptides. For each peptide fragment detected in LC-MS, the mass was assigned to a fragment of the respective parent peptide (Figure 4B). This analysis indicated that the marmoset sequence gets rapidly degraded by cleavage in the middle of the T-cell epitope, between the Phe_{44} and Ser_{45} residues. This is followed at a slower rate by a cleavage after Tyr_{40}. The presence of the Pro_{42} residue in the human sequence (instead of Ser_{42} in the marmoset sequence) seems to completely abrogate these cleavage sites, instead preferring two more productive cleavage sites on the C-terminal end of the sequence.

In conclusion, the unexpected T-cell activation by the cross-presentation of $hMOG_{35-55}$-$Cit_{46,52}$, in comparison to the immunologically inactive $mMOG_{35-55}$-$Cit_{46,52}$ remains not fully explained. The observed cross-reactivity for $hMOG_{35-55}$-$Cit_{46,52}$ in $hMOG_{35-55}$ marmosets is however quite interesting, as this is in contrast with the findings in a similar murine model,[17] where $mMOG_{35-55}$ immunized mice did not show cross-reactivity with $mMOG_{35-55}$-Cit_{46}. Further study of the biophysical and biochemical differences between these peptides is therefore necessary for the development of better animal models of multiple sclerosis.

However, these experiments and the experiments described in Chapter 3, as well as most work on the citrullination of MOG, have been carried out on peptide level. It is expected that substantial differences between the wild-type and (site-specifically) citrullinated protein could exist. Non-site-specifically citrullinated proteins can be generated *in vitro* by treatment with recombinant peptidyl arginine deiminase (PAD) enzymes, but these would not enable the study of the exact role of different citrullination sites. Alternatively, chemical or chemoenzymatic semi-synthesis of the entire protein would be able to generate site-specifically modified material. Here, synthetic peptides are ligated together using either native chemical ligation (NCL)[20,21] or enzymatic ligation to produce native amide bonds. These types of approaches enable peptide chemists to get around the typical limitations of synthetic peptide chemistry, which usually is limited to the synthesis of peptides <50 amino acids, to produce longer peptides and (small) proteins. Both of these methods involve the ligation of unprotected synthetic peptides to synthetic or expressed protein fragments in aqueous buffer. However, both methods differ in the functional requirements of the fragments that are to be ligated.

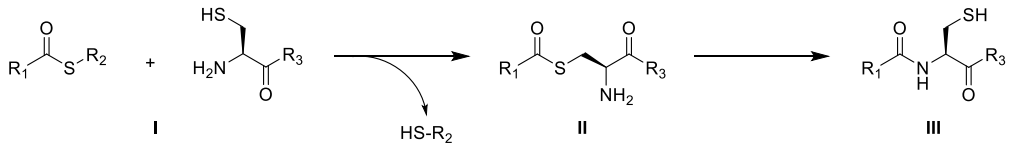

Figure 5. General mechanism of native chemical ligation. R_1 and R_3 denote two peptide chains, while R_2 denotes the thiol catalyst.

In native chemical ligation, a cysteine residue on the N-terminus of one peptide fragment reacts with a thioester on the C-terminus of the other (or the same, when cyclisation is desired). This nucleophilic attack of the cysteine thiol onto the carbonyl results (Figure 5, I) in a thioester exchange, producing intermediate II. The N-terminal amine of the cysteine can then perform a nucleophilic attack on the carbonyl, performing a S-to-N shift via a 5 membered ring transition state and forging a peptide bond, effectively condensing the two peptide fragments. However, cysteine is a quite rare amino acid in native human proteins (1.5-2.2% of all amino acids in the proteome)[22,23] and the requirement for this amino acid at the ligation site somewhat limits the application. To alleviate this, desulphurization chemistry was developed, enabling the conversion of cysteine residues into alanine. In this way, the scope of native chemical ligation reactions was expanded to more common alanine containing junctions.[24,25]

Here, the application of these approaches is evaluated for the synthesis of site-specifically citrullinated extracellular domain of MOG. Since the arginine residues of interest (Arg_{41}, Arg_{46}, Arg_{52}) are all in close proximity of each other and relatively close to the N-terminus of the protein, a semisynthetic approach was considered initially. This would involve the production of the C-terminal part of the protein using recombinant expression, while the N-terminal region would be produced synthetically. Only two cysteine residues are present in the sequence of MOG_{1-125}, one on position 24 and another on position 98. Neither of these are in a beneficial position for ligation with a peptide fragment that contains the desired citrulline replacements, so an alanine-to-cysteine replacement was considered instead. A viable ligation site was found between Gln_{61} and Ala_{62}, producing two fragments, MOG_{1-61} and $MOG_{62-125}A_{61}C$. The unnatural cysteine in position 62 can be removed post-ligation using a desulphurization reaction, reducing the residue to the natural alanine. This will, however, have the drawback of simultaneously reducing the natural Cys_{98} to alanine.

Looking at the SPPS based part of the route, the MOG_{1-61} peptide required for the N-terminal half of the protein is still on the large side for synthetic peptide chemistry. To alleviate this, a second disconnect between Pro_{23} and Cys_{24} was added, in order to reduce the complexity, and therefore potentially increase the yield, of the SPPS part of the route. To provide regioselectivity, the cysteine residue on the N-terminus of the MOG_{24-61} fragment will initially be protected as a thiazolidine, ensuring regioselectivity in the first ligation. This approach is outlined in Figure 6.

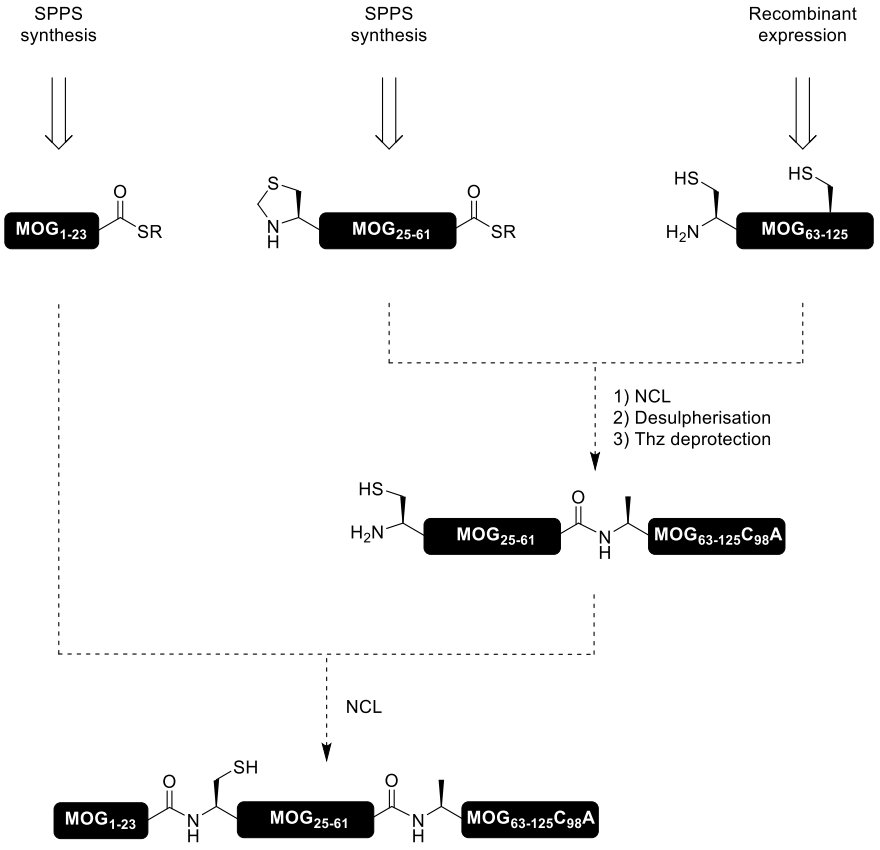

Figure 6. Initial semisynthetic approach towards MOG_{1-125}.

Since ligation on proline-thioesters is known to be difficult,[26] this ligation junction was evaluated first. The MOG_{1-23} peptide was synthesized bearing two different thioester surrogates on the C-terminus. Thioester surrogates are commonly used during the SPPS assembly of peptides for NCL, since thioesters themselves are not stable to all steps in Fmoc-SPPS (i.e. Fmoc deprotection with piperidine/DMF).[27] MOG_{1-23} was synthesized bearing either the bis(2-sulfanylethyl)amido (SEA)[28] (**1**) or *N*-acyl-benzimidazolinone (NBz)[29] (**2**) group on the C-terminus. Both of these were ligated under various different conditions with a test peptide consisting of the first six amino acids after the ligation junction (MOG_{24-29}, **3**). These experiments (Figure 7A) showed that the NBz thioester surrogate **2** shows the most promise for this thioester junction. The optimal conditions were 6 M guanidine in 200 mM NaPi buffer, pH 7.0, with 200 mM mercaptophenylacetic acid (MPAA) as thiol catalyst and 50 mM triscarboxyethylphosphine (TCEP).

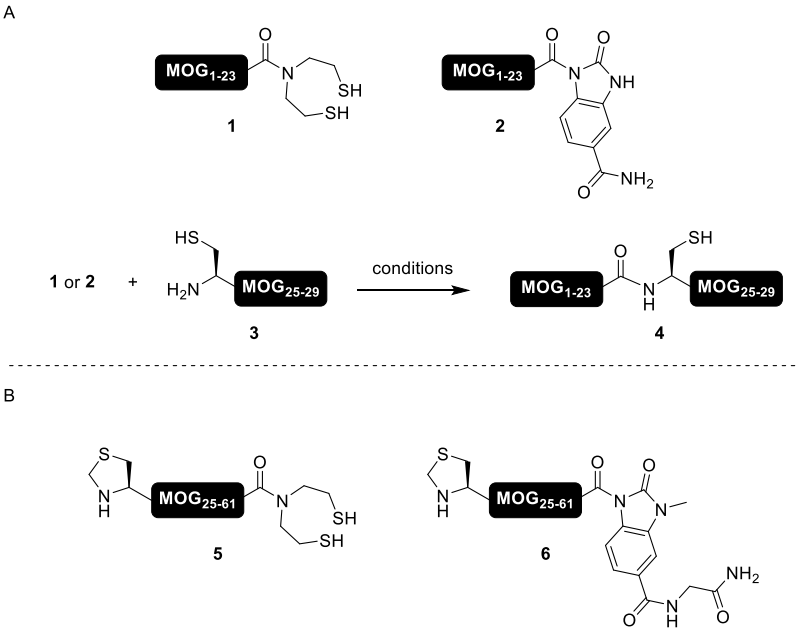

Figure 7. A) MOG_{1-23} peptide as a C-terminal SEA (**1**) and NBz (**2**) derivative and the test ligations performed on these peptides with MOG_{24-29} (**3**). B) Structure of the C-terminal SEA (**5**) and MeNBz (**6**) derivatives of MOG_{24-61}.

The synthesis of the middle fragment (MOG_{24-61}) was initialized on solid support containing the SEA linker using, after the loading of the first amino acid, standard Fmoc-SPPS conditions. LC-MS analysis of the crude peptide indicated a multitude of monodehydrated (Δm = -18 Da) or bisdehydrated (Δm = -36 Da) species, which were assumed to be the result of aspartimide formation.[30] Dimethoxybenzyl protection[31] of the peptide backbone at the $Aps_{58}Gly_{59}$ dipeptide was applied, which limited but not abolished the aspartimide formation. When, as an additional measure, a small percentage (1% (v/v)) of formic acid was introduced into the Fmoc deprotection solution (20% (v/v) piperidine in DMF), as described by Michels *et al.*,[32] this side reaction was fully suppressed, allowing synthesis of SEA peptide **5**. To evaluate a different latent thioesters for this ligation reaction, the MOG_{24-61} peptide was also synthesized as an *N*-acyl-*N'*-methyl-benzimidazolinone (MeNBz)[33] thioester surrogate (**6**). However, the

MeNBz acylurea moiety was found to be unstable on this peptide during RP-HPLC purification, resulting in contamination of the isolated peptide with hydrolyzed peptide, and this option was abandoned.

For the expression and subsequent purification of the $MOG_{62\text{-}125}A_{62}C$ fragment (**7**), a construct was created bearing a His_6-tag followed by a TEV cleavage site at the N-terminal site of the peptide. The His-tag would aid purification of the peptide, while the TEV cleavage site would enable liberation of the N-terminal cysteine required for ligation. While expression and purification of this protein fragment could be conducted without incident, removal of the His-tag via TEV cleavage did not proceed as planned. After addition of the TEV protease, disappearance of the protein construct was observed by both SDS-PAGE and LC-MS, but the cleaved fragment was not observed. The was assumed to be caused by a lack of solubility of the fragment in the protease buffer. This, combined with a concern about the importance of the Cys_{98} residue, shown to form a disulfide bond with Cys_{24},[34] that would be mutated to alanine using this approach, instigated an investigation into alternative synthetic routes.

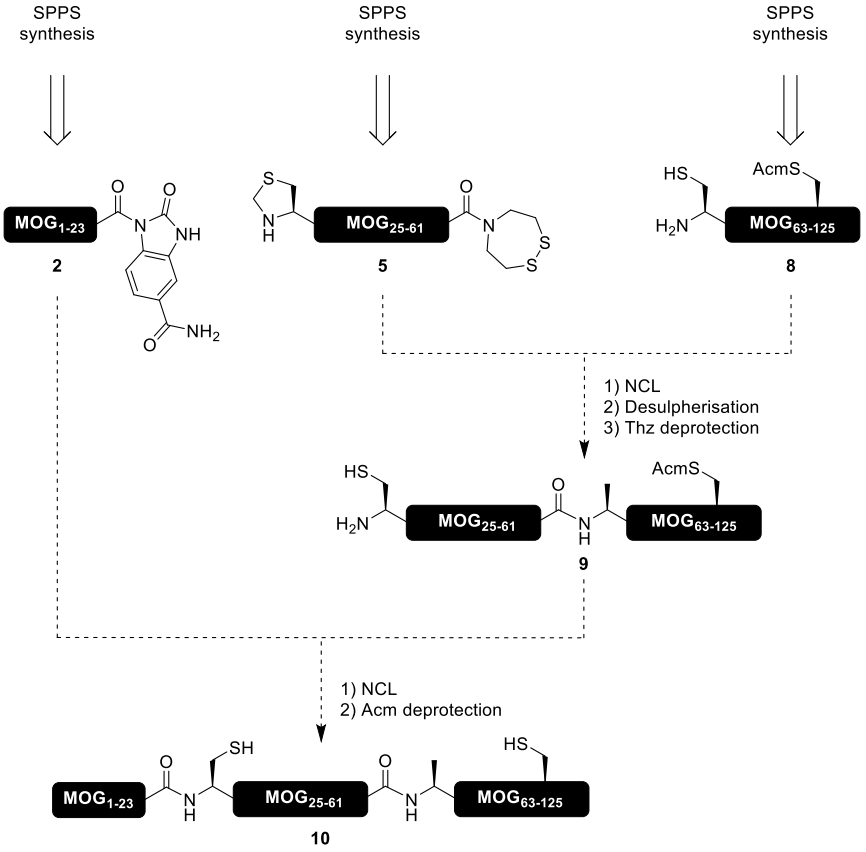

Figure 8. Proposed synthesis of $MOG_{1\text{-}125}$ utilizing three synthetic peptides and two ligation steps.

First, a chemical synthesis based on the already designed semisynthetic approach was considered (Figure 8), producing the $MOG_{62\text{-}125}A_{62}C$ fragment using SPPS instead of recombinant expression. This would allow the incorporation of an acetamidomethyl (Acm) protecting group on Cys_{98}, facilitating selective desulfurization of Cys_{62}. However, at 64 residues, this peptide would be outside the range of easily synthesizable peptides. In an

attempt to synthesize this long peptide, all amino acid couplings were carried out as double couplings, that is repetition of the coupling cycle before Fmoc deprotection. Additionally, pseudoproline protected dipeptides[35] were applied on the $Phe_{96}Thr_{97}$ and $Val_{81}Thr_{82}$ positions, which have been used to great effect during the chemical synthesis of other long peptides.[36] However, even when combining all of these techniques, the quality of the crude peptide was poor and the desired $MOG_{62\text{-}125}A_{62}C$ (**8**) could not be isolated.

In order to simplify the solid support synthesis of the peptides, an additional NCL disconnect between Thr_{97} and Cys_{98} was envisioned (Figure 9). While this simplification of the peptide synthesis should allow for easier purification and higher yields of the peptide fragments, this comes at the cost of additional steps during the assembly of the protein. To facilitate facile desulfurization of Cys_{62}, that is without the need for additional protecting group manipulations, the ligation between fragment **11** and **12** was selected as the first ligation. This required an inert latent thioester on the C-terminus of this fragment, for which a hydrazide function was selected.[37] Since the activation of the hydrazide function requires low pH, the thiazolidine group used previously as N-terminal protection for peptide **5** would no longer be orthogonal. An Acm group was chosen instead as an orthogonal protective group for the N-terminal cysteine in peptide **11**.

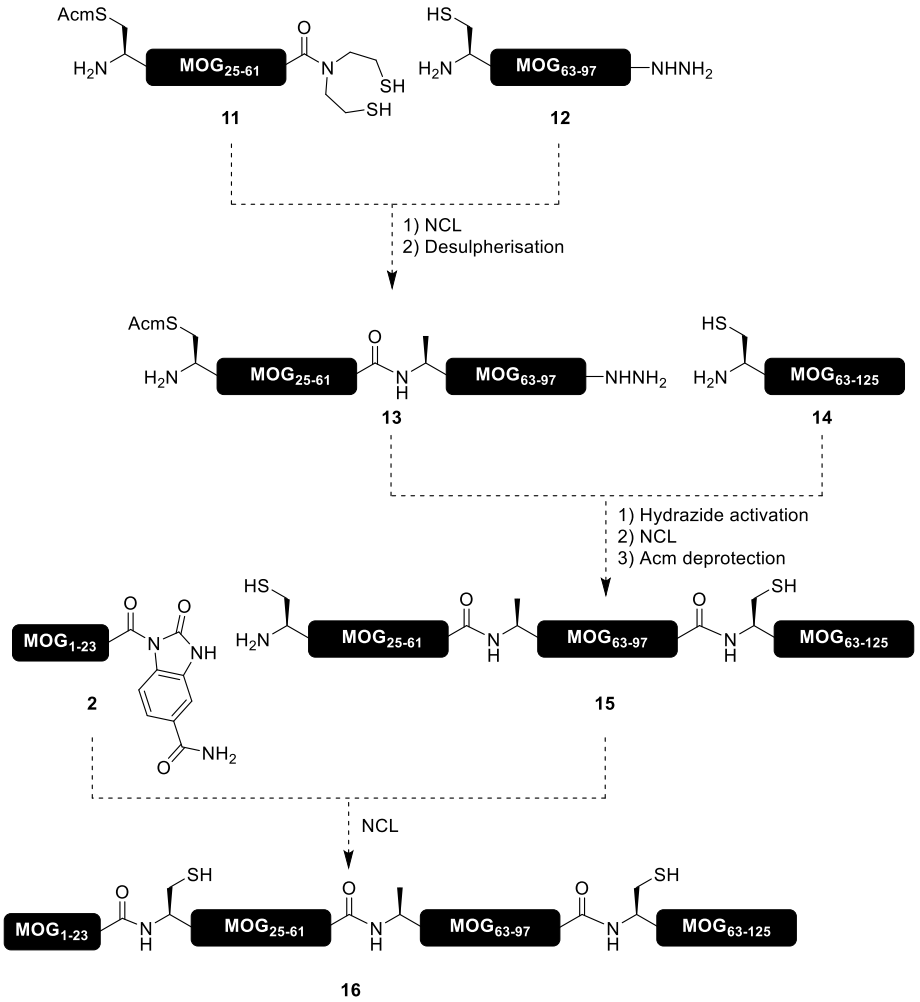

Figure 9. Total chemical synthesis of MOG1-125 using a four peptide three ligation approach. All peptides (**2**, **11**, **12** and **14**) were produced synthetically using SPPS.

Synthesis of all four of these peptides proceeded smoothly, and the ligation of fragments **11** and **12** was evaluated. For NCL reactions, the usual catalyst is the thiophenyl derivative MPAA. However, aromatic thiols have been shown to negatively interfere with the radical desulfurization chemistry.[38] Therefore, alternative catalysts have been proposed to enable one-pot ligation-desulfurization approaches. The most promising of these catalysts is trifluoroethanethiol (TFET),[39] and the ligation reaction was first evaluated using this catalyst, using **5** instead of **11** (Figure 10). Regrettably, only a small amount of ligation was observed, with both starting peptides showing significant degradation. As an alternative, a ligation reaction using a concentration of MPAA lower than normal was considered. This smaller amount of MPAA could then be removed using diethylether washes, potentially enabling one-pot ligation-desulfurization, although in a more laborious manner. These reactions seemed to proceed more effectively, with around 50% conversion observed after 24h. Oxidation, both in the form of disulfide formation with MPAA as well as methionine oxidation, was however a major side reaction.

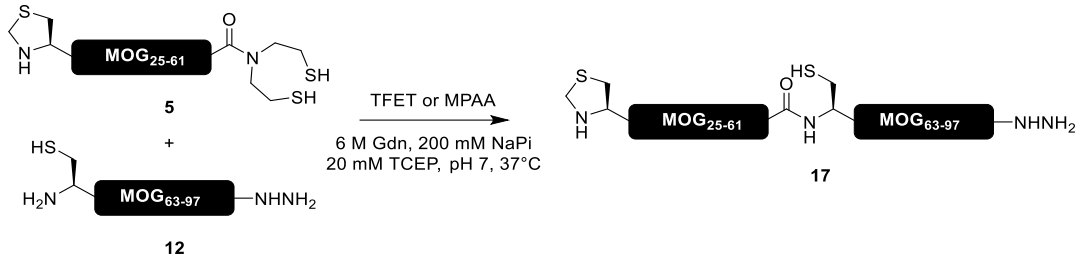

Figure 10. Attempted ligation of fragments **5** and **12**. Both TFET and MPAA were evaluated as thiol catalysts for this ligation.

As a third and final attempt, a chemoenzymatic ligation approach was considered. For this, Omniligase-1,[40] an enzyme capable of catalyzing the ligation between a peptide ester and a free N-terminus, was applied. This enzyme is an example of the class of peptide ligases, which were recently reviewed by Nuijens *et al*.[41] Omniligase itself is an modified form of another ligase enzyme, Subtiligase, engineered to broaden the substrate scope. As the name implies, the resulting enzyme has a broad substrate sequence scope for both the peptide ester and the amine fragment. Furthermore, it also has an improved S/H ratio, that is the ratio between productive ligation and peptide ester hydrolysis. Because of these features, Omniligase-1 is under active investigation as the enzyme of choice for chemo-enzymatic peptide synthesis (CEPS) of pharmaceutical peptides, like the GLP-agonist peptide exenatide.[42]

For the chemoenzymatic synthesis of $MOG_{1\text{-}125}$, a strategy using a single disconnect was considered optimal, as this would circumvent laborious protecting group manipulations. Since no PTMs are desired in the C-terminal fragment of the protein, a semisynthetic approach was taken. As for the ligation junction, the $Val_{47}Val_{48}$ junction was chosen, as the ligase has been shown to prefer aliphatic amino acids on both the C-terminal and N-terminal side of the ligation junction.[43] There are however two downsides to this ligation junction: i) it removes the ability to study citrullination of Arg_{52}, and ii) the critical Arg_{46}Cit modification would be in the P2 pocket of the ligase. Since the tolerance of the enzyme towards of citrulline residues inside the enzyme pocket has not previously been tested, this had to be evaluated before synthesis of the full protein could be attempted.

The tolerance of the enzyme for citrulline in P2 was evaluated by a test ligation between $MOG_{48\text{-}53}$ (VHLYRN) as the nucleophilic fragment and $MOG_{43\text{-}47}$ (PFSXV, with X = Arg or Cit) C-terminally functionalized with a carboxyamidomethyl-leucine (OCamL) ester, the preferred C-terminal ester of Omniligase-1.[44] The N-terminal proline on the $MOG_{43\text{-}47}$ fragments prevents homoligation, ensuring that the ligated $MOG_{43\text{-}53}$ fragment and hydrolysis of the Cam ester are the only observed products. Under these conditions, both ligations show full consumption of the peptide ester fragment in two hours (Figure 11). For arginine containing ester **18**, a S/H (Synthesis/Hydrolysis) ratio of 2.0 was observed. The ratio was slightly worse for citrulline containing peptide **19** at 1.6. While these ratios are not as high as those obtained with other peptide esters tested with Omniligase-1, this result does indicate that citrulline is tolerated in the P2 pocket, potentially enabling the synthesis of the desired citrullinated MOG protein, as well as other citrullinated proteins.

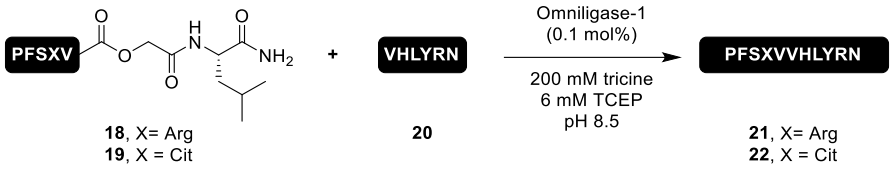

Figure 11. Test ligation reactions to determine the tolerance for citrulline in the P2 pocket of omniligase-1.

Next, the MOG_{48-125} fragment required for the ligation was expressed. This fragment was initially expressed C-terminally fused to a TEV cleavage site, followed by His_6 extension, creating the MOG_{48-125}-TEV-His_6 fusion protein **24**. This polypeptide was expressed and purified in a similar manner as the His_6-TEV-$MOG_{62-125}A_{62}C$ polypeptide (**7**) described above. Removal of the His-Tag via TEV protease was left for a later stage, since a C-terminal modification should not interfere with the ligation experiments. For the peptide ester part of the ligation, a peptide covering the native sequence of MOG_{27-47}, C-terminally extended with OCam followed by LKK was synthesized (**23**). These extra C-terminal lysines are not required for the ligation, but are tolerated by the enzyme and could help solubility of the peptide ester. This fragment again contained an N-terminal proline, preventing homoligation.

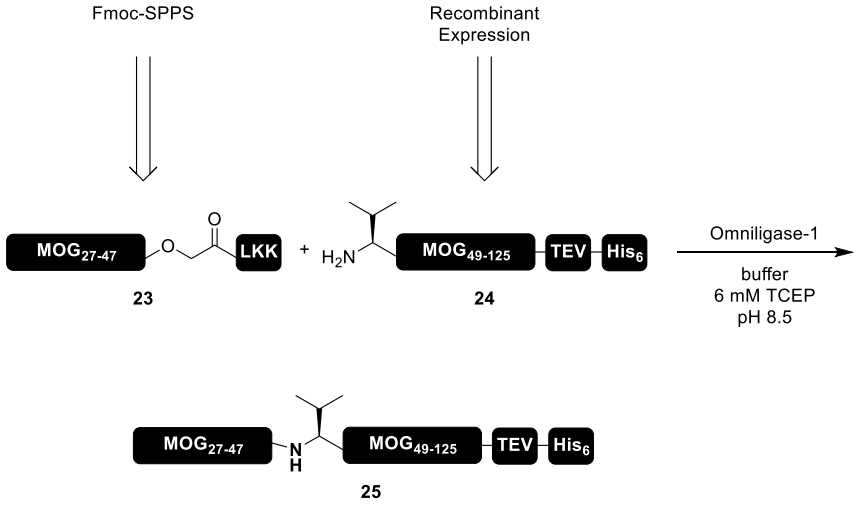

Figure 12. Test ligations with Omniligase-1 using expressed protein fragment **24** together with synthetic peptide **23**. A variety of different buffer compositions were tested, as outlined in table S1.

Since the protein fragment was expressed in inclusion bodies, solubilization with chaotropic agents was required. The protein could be solubilized with either 8 M urea or 6 M guanidine, with guanidine giving better recovery of protein. However, Omniligase-1 is hindered by the presence of chaotropic agents, and does not tolerate urea concentrations > 6 M or guanidine concentrations > 2 M.[43] Therefore, chaotrope concentrations were lowered after purification of the protein fragments by ultrafiltration over a 3 kDa molecular weight cut-off filter. Furthermore, both sodium phosphate and tricine buffers were evaluated, as the employed buffer salt can also influence the enzymatic ligation. For all conditions tested, complete consumption of peptide ester **23** was observed by LC-MS analysis after 4h. It was confirmed that this was primarily due to enzymatic hydrolysis, and not hydroxide mediated hydrolysis due to the high pH of the buffer, as incubation of peptide **23** in ligation buffer for up to 4 hours

yielded negligible hydrolysis. All ligation reactions were followed over time by LC-MS, at 0, 1, 2 and 4 hours. Since the peaks of polypeptide **24** and **25** did not separate on C18-column, conversion was estimated by SDS-PAGE analysis of the reaction mixtures after 4 hours. A complete overview of all ligation conditions is given in supplementary Table S1.

Briefly, while guanidine achieved the highest protein concentration and therefore the best conversion, a 2 M concentration was not enough to keep the protein soluble at room temperature. The same was found for 2 M urea, where also precipitation was observed. 4 M urea in tricine buffer was chosen as the best combination, with a compromise between protein solubility and ligase activity.

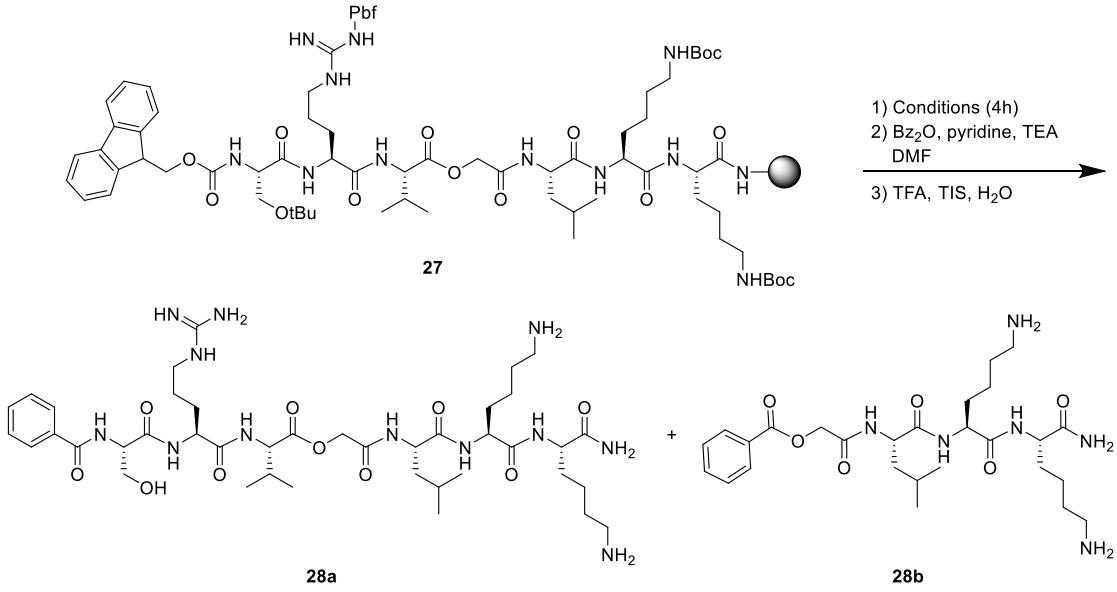

Figure 13. Demonstration of the experiment used to evaluated the stability of resin-bound ester **27** when treated with various Fmoc-deprotection conditions.

To evaluate the efficiency of these conditions for the semisynthesis of MOG_{1-125}, the synthesis of the N-terminal peptide MOG_{1-47}-OCamLKK (**26**) was required. To achieve a high quality crude product after SPPS, and therefore high yields of this substantial peptide, the SPPS needed to be properly optimized beforehand. The ester at the C-terminal side of the peptide could suffer from unintentional aminolysis (or hydrolysis if water is present) during the many Fmoc-deprotection steps required, especially at the elevated temperatures commonly used in microwave assisted peptide synthesis. A selection of commonly employed Fmoc-deprotection mixtures were tested on resin bound peptide **27**, consisting of the three C-terminal amino acids of MOG_{1-47} coupled to the OCamLKK ester. These deprotection solutions were tested at room temperature, 50°C and 90°C, in each case for 4 hours. After the removal of the deprotection solution, the resin was treated with a mixture of benzoic anhydride, pyridine and triethylamine in DMF, to benzoylate both the free amine and alcohol functions. Next, the peptides were liberated from resin with TFA (95:2.5:2.5, TFA/H_2O/TIS) and analyzed by LC-MS. Using this approach, the ratio of intact versus deacylated peptide was determined

by ratio of the peak areas as determined by LC-UV. An overview of the results is shown in Table 2.

Table 2. Overview of the effect of different deprotection conditions on the stability of the ester bond in immobilized peptide **27**. For each condition, the peak area of the peak assigned to **28a** is given as a percentage of the total peak area in the chromatogram. All percentages as given as volume percent (v/v) of the solution in DMF, except for piperazine which is given as a weight percentage instead (w/v). RT = room temperature, ND = not detected.

	Temperature		
Condition	RT	50°C	90°C
20% Piperidine	>95%	88%	25%
20% Piperidine + 1% CHOOH	>95%	95%	84%
5% Piperazine	>95%	>95%	42%
50% Morpholine	>95%	95%	43%
2% DBU	>95%	73%	ND

At 90°C, the standard 20% (v/v) piperidine in DMF solution is quite capable of cleaving the ester bond, even on a sterically hindered residue like valine. By buffering the solution with the addition of formic acid, this reaction can be almost completely suppressed. At 50°C, the ester bond is nearly completely retained, indicating that temperature is the most critical factor for this side reaction. At room temperature, nearly no cleavage of the peptide ester was observed for any of the deprotection solutions. Therefore, the synthesis of peptide **26** carried out using room temperature Fmoc-deprotection protocols in the automated peptide synthesizer. By using these conditions and a combination of manual and automated SPPS protocols, peptide **26** was isolated in 7% yield.

This peptide ester was then used in a test ligation with protein fragment **24**, using the same conditions as described for the test ligations with peptide **23**. However, during these reactions, both ligation and enzyme catalyzed hydrolysis proceeded exceptionally slow. Furthermore, peptide **23** was found to be unstable on storage, with, besides expected methionine oxidation, an unknown degradation product appearing upon prolonged storage. Therefore, further optimization of this ligation reaction is required before semisynthesis of $MOG_{1\text{-}125}$ can be achieved.

Chapter 4 describes the synthesis of a series of antigenic peptides bearing N-terminal glycoclusters and a C-terminal fluorophore. The antigen of choice is the well-studied ovalbumin-derived peptide $OVA_{247\text{-}264}$, containing the $CD8^+$ T-cell restricted epitope $OVA_{257\text{-}264}$. The fluorophore allows for the detection of the glycosylated peptides upon binding to a lectin, like the mannose receptor (MR), using a technique called glyco-PAINT.[3] By direct incorporation of the fluorophore onto the glycoconjugate antigen, the MR binding and uptake of these peptides can be directly measured using the glyco-PAINT technique. By combining

glycocluster, antigen and fluorophore into a single construct, the opportunity arrives to directly correlate MR binding with T-cell activation. This could contribute to the understanding of the effect glycosylation has on antigen cross-presentation, a topic of active research and debate.[4,45] Furthermore, the synthetic techniques used in this chapter could also be used for the generation of synthetic, glycosylated vaccine candidates.

Synthesis of these conjugate peptides did not proceed without problems. The oligosaccharides were introduced with copper catalyzed click chemistry (CuAAC) using propargylated glycans. To facilitate this conjugation, a series of azidolysine residues were included on the N-terminal side of the peptide. However, incorporation of multiple azidolysine residues critically lowered the solubility of the resulting peptides, severely hindering the following CuAAC reactions. To alleviate this, a flexible PEG based spacer was introduced between the N-terminus of the antigenic peptide and the glycocluster, greatly increasing solubility and enabling the synthesis several glycosylated peptides. Furthermore, determining the effect of the PEG spacer on the MR binding kinetics of the glycoconjugates could give valuable information for further design of antigen-glycocluster conjugates.

For further development in this area, peptides containing a $CD4^+$ T-cell restricted epitope could also be similarly decorated with glycocluster and fluorophore. A useful model epitope to consider here is the $OVA_{323-339}$ peptide for which, just like $OVA_{247-264}$, a variety of specific T-cell have been developed. Some initial explorations into these peptides were made, as shown in Figure 14A.

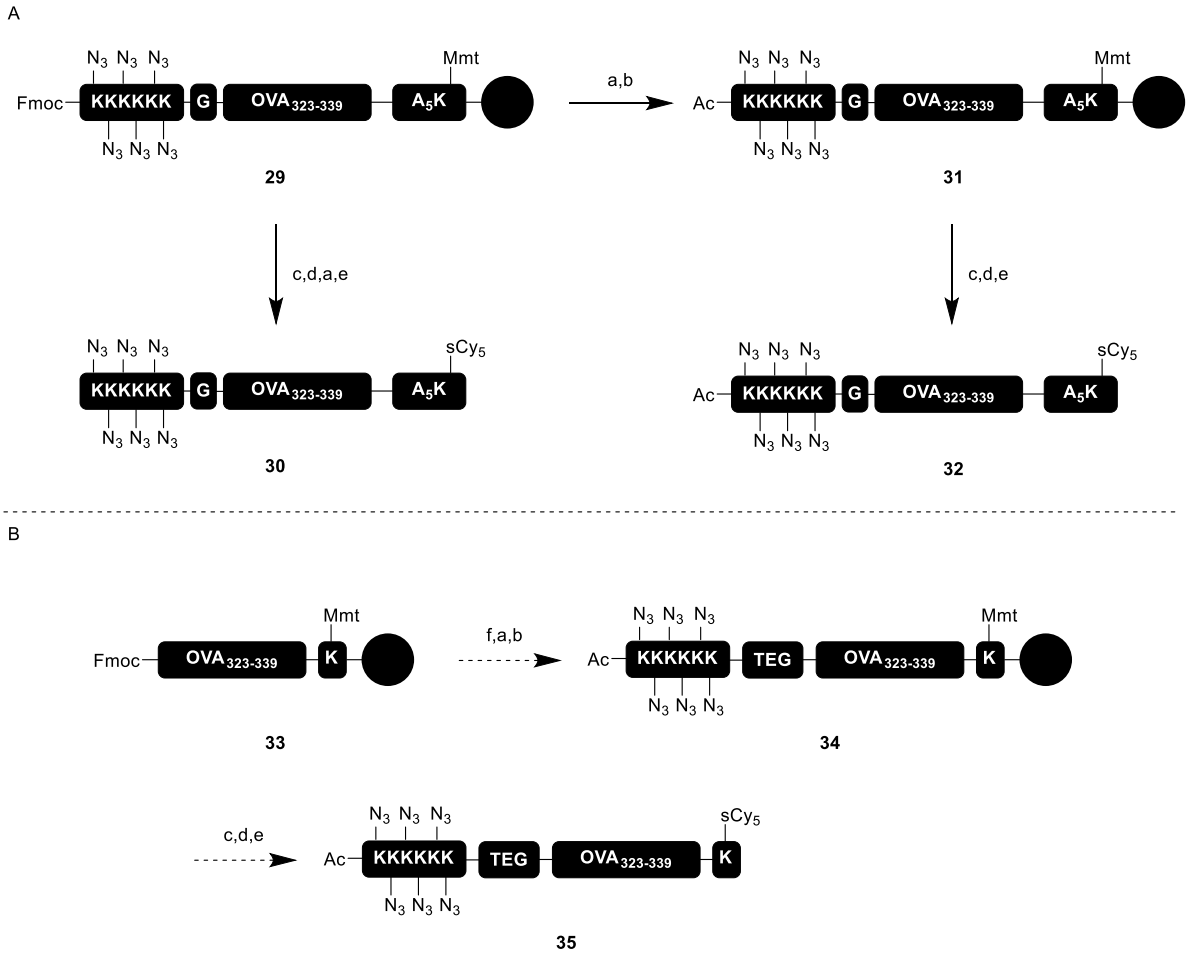

Figure 14. A) Failed synthesis of $OVA_{323-339}$ based model antigenic peptides **30** and **32**. B) Proposed synthesis of new $OVA_{323-339}$ model antigenic peptide **35**. Reagents and conditions: a) 20% (v/v) piperidine, DMF b) Ac_2O, DiPEA, DMF c) AcOH, TFE, DCM d) sCy5-OH, HCTU, DMF e) TFA, TIS, H_2O f) Fmoc-SPPS.

First, a similar approach to the $OVA_{247-264}$ based peptides was taken. The C-terminus of the epitope was extended with the amino acid sequence AAAAAK, the lysine bearing the highly acid labile Mmt protective group. N-terminally, the peptide was extended with a glycine residue, followed by six azidolysine residues. Using standard automated SPPS conditions, immobilized peptide **29** was obtained. The Mmt protective group was then selectively removed with AcOH and TFE in DCM. Next, the fluorophore was incorporated, using HCTU as a mediator. Finally, the N-terminal Fmoc was removed and the peptide liberated from the support. This yielded a very poor quality crude, with high amounts of double fluorophore modified material present, as well as many unidentified side products. Recovery of the desired peptide **30** from this mixture using RP-HPLC was unsuccessful. The issue of undesired over labeling of the N-terminus of the peptide was addressed by acetylation, as was done for the $OVA_{247-264}$ derived model peptide, to produce resin-bound peptide **31**. The C-terminal lysine was, after Mmt cleavage, again modified with fluorophore. After cleaving the peptide from the support, the level of fluorophore incorporation, however, was found to be low. Furthermore, the crude material was highly insoluble, making RP-HPLC challenging.

Instead, a new scaffold based around the $MOG_{323-339}$ peptide could be considered (Figure 14B). The synthesis would start from peptide **33**, removing the C-terminal penta-alanine spacer. N-terminally, the same TEG spacer using in chapter 4 could be incorporated between the N-terminus of the epitope and the azidolysine cluster (**34**). This combination of changes should hopefully increase solubility of the scaffold sufficiently to allow for efficient synthesis and purification of peptide **35**.

Chapter 5 outlines the synthesis of a cyclic, pentavalent scaffold conjugated with glycans via CuAAC chemistry. This scaffold consists of a series of six lysine residues, five used as carbohydrate attachment points. The sixth lysine was used to conjugate a fluorophore to the scaffold, creating a trackable, multivalent glycoconjugate. To realize this goal, a combination of on-resin chemistry, to build the scaffold, and off-resin conjugation reactions were used. To create the cyclic core of the molecule, on-resin cyclization of the peptide backbone was used, using a head-to-tail cyclization approach as has been reported many times in the literature. However, like in many other cases, on-resin dimerization during the cyclization phase was a major obstacle, resulting in very little product formation. The length of the linear peptide, which was significantly greater than the length of the typical linear peptide of most published cyclization reactions, seemed to play a major part here. By changing the design slightly, going from a 6-carbon to a 4-carbon spacer amino acid between the carbohydrate attachment points, the cyclization was carried out successfully. Next, long, polyethylene glycol (PEG) based spacers were introduced onto the five lysine residues. To accomplish this, all five of these residues needed to be deprotected without damaging the labile resin linkage. Using highly acid labile monomethoxytrityl groups in combination with a mildly acidic deprotection solution, very high conversion with good retention of the resin linker was achieved. Finally, CuAAC mediated glycan conjugation, using the methods from Chapter 4, followed by fluorophore labeling, produced the desired labeled glycoconjugates.

With this effective method in hand, glycoconjugates with different valencies can be produced in a straightforward manner, assuming the length of the peptide backbone won't interfere with the cyclization step. Since there are many tetravalent lectins with important functions in immunology, like DC-SIGN[46] and the cation-independent mannose-6-phosphate receptor (CI-MPR),[47] a tetravalent design would be an interesting next step. Using the chemistry developed in Chapter 5, such a ligand could be relatively straightforward to synthesize. A clickable ligand for the CI-MPR, bearing a non-hydrolyzable phosphonate on the 6-carbon of mannose was recently published.[48] This molecules, however, has an alkyne as the conjugation group, necessitating the design and synthesis of a scaffold bearing azide handles for the conjugation. The synthesis of these scaffolds is described in Figure 15.

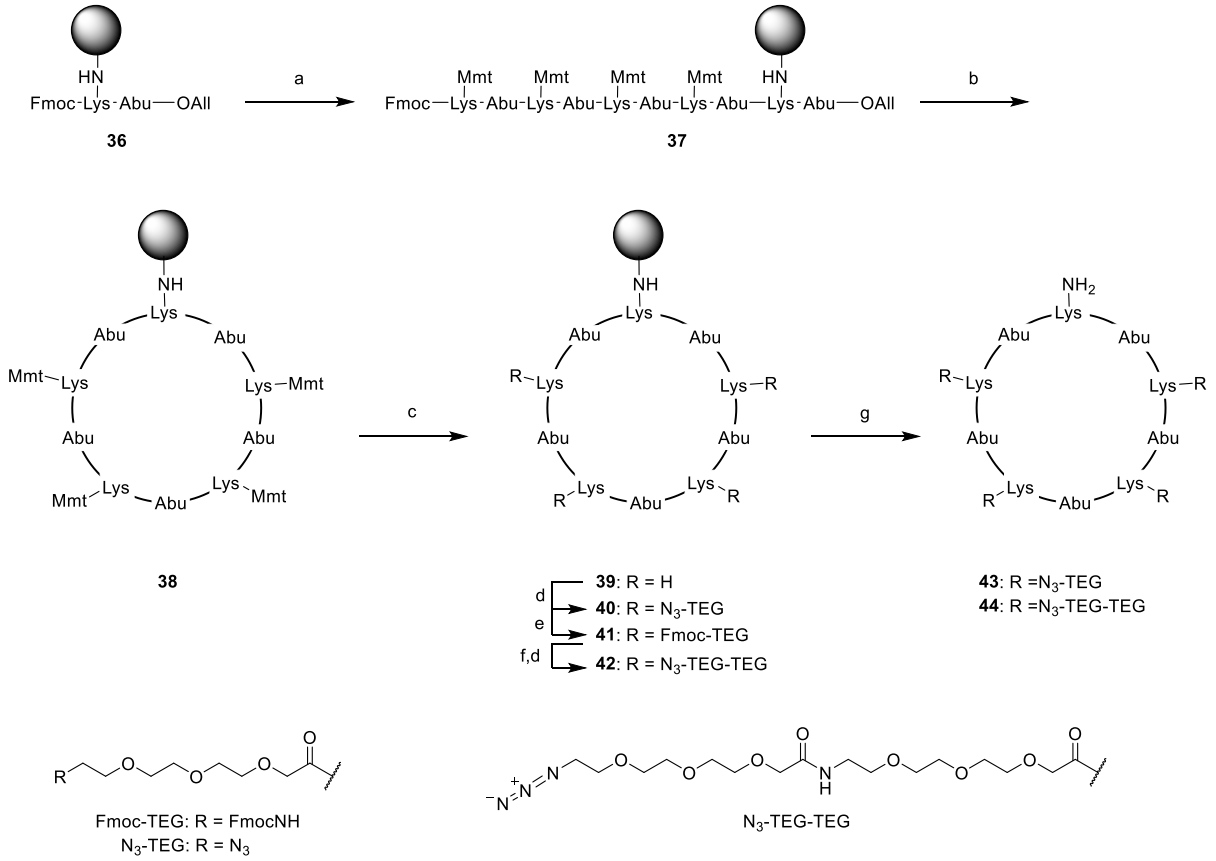

Figure 15. Synthesis of cyclic scaffolds **43** and **44** using the chemistry developed in Chapter 5. Reagents and conditions: a) Fmoc-SPPS b) i) $Pd(PPh_3)_4$, $PhSiH_3$, DCM ii) 2% (v/v) DBU, DMF iii) PyAOP, DiPEA, DMF c) AcOH, TFE, DCM d) N_3-TEG-OH, HCTU, DiPEA, DMF e) Fmoc-TEG-OH, HCTU, DiPEA f) 20% (v/v) piperidine, DMF g) i) TFA, H_2O, TIS ii) RP-HPLC (**43**: 9.8%), (**44**: 4.6%).

The synthesis started of as described in Chapter 5 from a dipeptide immobilized onto the solid support via a sidechain carbamate linkage (**36**). Standard Fmoc-SPPS conditions were used to elongate the peptide N-terminally (**37**). Using $Pd(PPh_3)_4$ and $PhSiH_3$ in DCM, the allyl ester was removed. After Fmoc deprotection using 2% (v/v) DBU in DMF, on-resin cyclization was carried out using PyAOP as the activator. Successful cyclization was confirmed by LC-MS analysis of a small portion of deprotected peptide, using the approach outlined in Chapter 5. The Mmt groups on immobilized peptide **38** were then removed using the AcOH/TFE cocktail (1:2:7 AcOH/TFE/DCM), producing immobilized cyclic peptide **39**. Since the requirements for good multivalent binding to CI-MPR are not known, two scaffolds with different lengths of spacer between the peptide backbone and the glycans were build. Half of **39** was acylated with N_3-PEG-OH, creating **40**. Acidic cleavage and RP-HPLC yielded **43** in 9.8% yield. The other half of **39** was first coupled with Fmoc-TEG-OH, producing **41**. The Fmoc-group was removed under standard conditions and N_3-TEG-OH was coupled, producing **42**. This compound was also released from the resin and purified, yielding **44** in 4.6% yield. The conjugation of these scaffolds with the mannose-6-phosphate ligand and a fluorophore remains to be explored.

Chapter 6 described development of a novel method for the synthesis of peptides containing a lysine residue protected with an allylic TCO group. Since TCO groups are rather sensitive to acidic conditions, direct Fmoc-SPPS synthesis of these peptides using, a TFA based global deprotection step, is not feasible. The novel approach involves the use of azide groups to mask all additional amines in the peptide (*i.e.* the N-terminus as well as additional lysine residues in the sequence). After global deprotection, the allylic TCO is introduced using an activated TCO carbonate. Following successful introduction of the modification, all azides are reduced to the corresponding amines using a Staudinger reduction with trimethylphosphine. This enables the synthesis of longer, TCO-caged peptides, containing multiple lysine residues. Furthermore, by not relying on a nucleophilic base-labile protecting group, like earlier works have done,[5,49] functions labile to nucleophilic base could also be introduced to the molecule, as was exemplified by the synthesis of a TCO-caged peptide containing a fatty acid ester.

Experimental

General methods for automated SPPS

Peptides were synthesized using automated Fmoc-SPPS on a Liberty Blue^{tm} automated microwave peptide synthesizer (CEM corporation). Synthesis was performed on a 100 µmol scale on Tentagel S RAM resin (loading 0.20-0.25 mmol/g, Rapp Polymere GmbH, Germany), unless stated otherwise. Resin was first swollen for 5 minutes in DMF prior to amino acid coupling. Activation was achieved using DIC/Oxyma coupling as is recommended by the manufacturer. The following amino acids were used: Fmoc-Ala-OH, Fmoc-Arg(Pbf)-OH, Fmoc-Asn(Trt)-OH, Fmoc-Asp(OtBu)-OH, Fmoc-Cit-OH, Fmoc-Cys(Acm)-OH, Fmoc-Cys(Trt)-OH, Fmoc-Gln(tBu)-OH, Fmoc-Glu(OtBu), Fmoc-Gly-OH, Fmoc-His(Boc)-OH, Fmoc-Ile-OH, Fmoc-Leu-OH, Fmoc-Lys(Boc)-OH, Fmoc-Met-OH, Fmoc-Phe-OH, Fmoc-Pro-OH, Fmoc-Ser(tBu)-OH, Fmoc-Thr(tBu)-OH, Fmoc-Trp(Boc)-OH, Fmoc-Tyr(tBu)-OH, Fmoc-Val-OH and Boc-Thz-OH. All amino acids were obtained from Novabiochem or Sigma Aldrich. Standard coupling was achieved using 5 equivalents amino acid as a 0.2 M amino acid/DMF solution, 5 equivalents DIC as a 0.5 M of DIC/DMF solution and 5 equivalents Oxyma as a 1 M Oxyma/DMF solution (also containing 0.2 M DiPEA), at 90°C for 2 minutes. Standard Fmoc deprotection was achieved by 20% (v/v) piperidine in DMF at 90°C for 90 seconds, repeated once. For peptide **5**, **6** and **11**, 1% (v/v) of formic acid was added to the deprotection solution and the Fmoc deprotection was carried out at room temp for 2 x 5 min instead. To analyze the quality of a resin bound peptide, a small amount of resin (~1mg) was treated with 200 µL of a TFA cocktail (95:2.5:2.5, TFA/H_2O/TIS) for 2 hours, after which the TFA was filtered into 800 µL of ice cold Et_2O. After five minutes the formed precipitate was collected by centrifugation and the supernatant discarded. The pellet was dissolved in 200 µL 1:1:1 H_2O/MeCN/tBuOH and subjected to LC-MS analysis. Peptides were characterized using electrospray ionization mass spectrometry (ESI-MS) on a Thermo Finnigan LCQ Advantage Max LC-MS instrument with a Surveyor PDA plus UV detector on an analytical C18 column (Phenomenex, 3 µm, 110 Å, 50 mm × 4.6 mm) in combination with buffers A (H_2O), B (MeCN), and C (1% aq TFA). Quality of crude was evaluated with a linear gradient of 10-90% B with a constant 10% C over 10 minutes. For mass analysis of peptides by low-resolution mass spectrometry (LRMS), calculated masses (calcd) were based on the most abundant isotopic pattern.

General methods for manual SPPS

Manual elongation of peptides was carried out in a fritted syringe at either 25 or 5 µmol scale. Fmoc deprotection was achieved using 20 % (v/v) piperidine in DMF in two steps, reacting 3 and 7 minutes respectively. Fmoc-Gly-OH was coupled using 5 equivalents of amino acid together with 5 equivalents of HCTU (as a 0.5 M solution) and 10 equivalents DiPEA for 45 minutes. Analysis of the quality of the resin-bound peptide was carried out as above.

General methods for resin cleavage and RP-HPLC purification

Global deprotection and resin cleavage of peptides was accomplished using a 95:2.5:2.5 mixture of TFA/TIS/H_2O for 3 hours, or a 90:2.5:2.5:2.5:2.5 mixture of TFA/Me_2S/thioanisole/H_2O/TIS for peptides containing a free cysteine, followed by precipitation from cold diethyl ether (1:9 ratio TFA to ether) and recovery of the precipitate by centrifugation. Crude, tryptophan containing peptides were

dissolved in MilliQ water and lyophilized overnight in order to remove the residual carboxylate. Preparative reverse phase HPLC on a Waters AutoPurification system (eluent A: H_2O + 0.2% TFA; eluent B: ACN) with a preparative Gemini C18 column (5 µm, 150 x 21.2 mm) yielded the final products after lyophilization. Quality of purified peptides was determined using a Thermo Scientific Vanquish UHPLC coupled to a Thermo Scientific LCQ Fleet ion trap electron spray ionization mass spectrometer (ESI-MS) using an analytical C18 column (Phenomenex, 3 µm, 110 Å, 50 mm × 4.6 mm) in combination with buffers A (H_2O), B (MeCN), and C (1% aq TFA). Quality of the peptides was evaluated with a linear gradient of 10-50% B with a constant 10% C over 9 minutes or a linear gradient of 5-65% B with a constant 10% C over 30 minutes.

Yields and analysis of peptides described in Table 1

Table 3. Overview of all synthesized peptides. [a] synthesis was previously described in Araman *et al.*[2]

Name	Sequence	Expected mass [M+2H]	Found mass [M+2H]	Yield (%)
mMOG$_{40-48}$-Cit$_{41}$	Y*Cit*SPFSRVV-OH	556.3	556.5	31.0
mMOG$_{40-48}$-Cit$_{46}$	YRSPFS*Cit*VV-OH	556.3	556.4	29.0
mMOG$_{40-48}$-Cit$_{41,46}$	Y*Cit*SPFS*Cit*VV-OH	556.8	556.9	32.7
mMOG$_{39-49}$-Cit$_{46}$	WYRSPFS*Cit*VVH-OH	718.3	718.1	17.2
mMOG$_{38-50}$-Cit$_{46}$	GWYRSPFS*Cit*VVHL-OH	803.4	803.2	26.8
mMOG$_{37-51}$-Cit$_{46}$	VGWYRSPFS*Cit*VVHLY-OH	934.6	934.5	27.4
mMOG$_{36-52}$-Cit$_{46}$	EVGWYRSPFS*Cit*VVHLYR-OH	1077.3	1077.1	13.3
mMOG$_{36-52}$-Cit$_{46,52}$	EVGWYRSPFS*Cit*VVHLY*Cit*-OH	1077.7	1077.6	27.2
mMOG$_{35-53}$-Cit$_{46,52}$	MEVGWYRSPFS*Cit*VVHLY*Cit*-OH	1200.4	1200.1	27.4

Experimental for MOG (semi)synthesis

Gly-Gln-Phe-Arg-Val-Ile-Gly-Pro-Arg-His-Pro-Ile-Arg-Ala-Leu-Val-Gly-Asp-Glu-Val-Glu-Leu-Pro-SEA (1)

500 µmol Tentagel PS chlorotrityl resin (1,44 µmol/g) was loaded with SEA linker in a 1:10 ratio followed by capping, as described by Ollivier et al.[28] This was followed by coupling of Fmoc-Pro-OH using 10 eq. amino acid and 9.5 eq HATU (as 0.5 M solution in DMF) together with 20 eq. DiPEA for one hour. Capping of unreacted secondary amines was carried out using a solution containing 10% (v/v) Ac_2O and 5% (v/v) DiPEA in DMF for 10 minutes, repeated once. An Fmoc loading test was carried out,[50] and loading was determined to be 0.12 mmol/g. The peptide was then further synthesized using the general manual SPPS conditions. Global deprotection followed by RP-HPLC purification yielded compound **1** as a white solid (11.5 mg, 4.3 µmol, 10%) **LC-MS** RT = 4.1 min (C18, 10-90% B over 9 minutes) **LRMS** calcd $[M+2H]^{2+}$ = 1337.7, $[M+3H]^{3+}$ = 892.5 observed M/z = 1338.1, 892.5

Gly-Gln-Phe-Arg-Val-Ile-Gly-Pro-Arg-His-Pro-Ile-Arg-Ala-Leu-Val-Gly-Asp-Glu-Val-Glu-Leu-Pro-NBz (2)

Dawson DBz AM resin (100 µmol, 0.47 mmol/g), preloaded with the diaminobenzamide (DBz) linker,[29] was acylated with Fmoc-Pro-OH using 5 equivalents of amino acid, 4.9 equivalents HATU (as a 0.5 M HATU solution in DMF) and 11 equivalents DIPEA for 90 minutes. The peptide was then further synthesized using the general manual SPPS conditions. To form the urea function of the NBz moiety, the Fmoc-protected resin was first treated with 5 equivalents of p-nitro-choloroformate in degassed DCM (0.25 M) for one hour. This was followed, after thorough washing, by treatment of the resin with a solution of N-methylmorphline (NMM) in DMF (0.5M) for 2 hours at 60°C. Global deprotection followed by RP-HPLC purification yielded compound **2** as a white solid (10.7 mg, 3.9 µmol, 3.9%) **LC-MS** RT = 14.2 min (C18, 5-65% B over 30 minutes) **LRMS** calcd $[M+2H]^{2+}$ = 1357.8, $[M+3H]^{3+}$ = 905.5 observed M/z = 1358.3, 906.0

Cys-Arg-Ile-Ser-Pro-Gly-NH_2 (3)

Peptide was synthesized on a 100 µmol scale on Tentagel S RAM resin using the standard condition for manual SPPS. Global deprotection followed by RP-HPLC purification yielded compound **3** as a white solid (46.3 mg, 73.4 µmol, 73%) **LC-MS** RT = 3.4 min (C18, 10-90% B over 9 minutes) **LRMS** calcd $[M+H]^{+}$ = 631.3 observed M/z = 631.4

Thz-Arg-Ile-Ser-Pro-Gly-Lys-Asn-Ala-Thr-Gly-Met-Glu-Val-Gly-Trp-Tyr-Arg-Pro-Pro-Phe-Ser-Arg-Val-Val-His-Leu-Tyr-Arg-Asn-Gly-Lys-Asp-Gln-Asp-Gly-Asp-Gln-SEA (5)

500 µmol Tentagel PS chlorotrityl resin (1,44 µmol/g) was loaded with SEA linker in a 1:10 ratio followed by capping, as described by Ollivier et al.[28] This was followed by coupling of Fmoc-Gln(Trt)-OH using 10 eq. amino acid and 9.5 eq HATU (as 0.5 M solution in DMF) together with 20 eq. DiPEA for one hour. Capping of unreacted secondary amines was carried out using a solution containing 10% (v/v) Ac_2O and 5% (v/v) DiPEA in DMF for 10 minutes, repeated once. The peptide was then further synthesized using the general automated SPPS conditions, using the formic acid containing Fmoc deprotection solution (1:20:79 CHOOH/piperidine/DMF). The $Asp_{58}Gly_{59}$ dipeptide was incorporated as the Fmoc-Asp(OtBu)-(Dmb)Gly-OH dipeptide building block. Global deprotection followed by RP-HPLC purification yielded compound **5** as a white solid (31.6 mg, 7.1 µmol, 14%). **LC-MS** RT = 13.8 min (C18, 5-65% B over 30 minutes) **LRMS** calcd $[M+3H]^{3+}$ = 1489.7, $[M+4H]^{4+}$ = 1117.5 observed M/z = 1489.4, 1117.4

Thz-Arg-Ile-Ser-Pro-Gly-Lys-Asn-Ala-Thr-Gly-Met-Glu-Val-Gly-Trp-Tyr-Arg-Pro-Pro-Phe-Ser-Arg-Val-Val-His-Leu-Tyr-Arg-Asn-Gly-Lys-Asp-Gln-Asp-Gly-Asp-Gln-MeNBz-Gly-NH_2 (6)

Peptide **6** was synthesized on a 100 µmol scale on Tentagel S RAM resin. The initial Gly residue was coupled manually, followed by manual coupling of the MeDBz linker, using 5 equivalents of Fmoc-MeDbz-OH, 5 equivalents HCTU as a 0.5 M HCTU/DMF solution and 5.5 equivalents DIPEA for 1 hour. Following Fmoc deprotection, Fmoc-Gln(Trt)-OH was coupled using 5 equivalents of amino acid, 4.9 equivalents HATU (as a 0.5 M HATU solution in DMF) and 11 equivalents DIPEA for 90 minutes. The peptide was then further synthesized using the general automated SPPS conditions, using the formic acid containing Fmoc deprotection solution (1:20:79 CHOOH/piperidine/DMF). The $Asp_{58}Gly_{59}$ dipeptide was incorporated as the Fmoc-Asp(OtBu)-(Dmb)Gly-OH dipeptide building block. Transformation of the MeDBz group into the MeNBz group was carried out as described by Blanco-

Canosa *et al.*[33] Global deprotection followed by RP-HPLC purification yielded 25.6 mg of peptide **6** as an inseparable mixture with the hydrolyzed peptide. **LC-MS** RT = 6.2 min (C18, 10-90% B over 9 minutes) **LRMS** calcd $[M+3H]^{3+}$ = 1527.1, $[M+4H]^{4+}$ = 1145.6 observed M/z = 1527.0, 1145.5. The co-eluting hydrolyzed peptide was also detected: calcd $[M+3H]^{3+}$ = 1450.0, $[M+4H]^{4+}$ = 1087.8 observed M/z = 1450.3, 1088.0.

Cys-Pro-Glu-Tyr-Arg-Gly-Arg-Thr-Glu-Leu-Leu-Lys-Asp-Ala-Ile-Gly-Glu-Gly-Lys-Val-Thr-Leu-Arg-Ile-Arg-Asn-Val-Arg-Phe-Ser-Asp-Glu-Gly-Gly-Phe-Thr-$NHNH_2$ (12)

2-Chlorotrityl chloride resin (200 µmol, 1.36 mmol/g) was modified with hydrazine monohydrate as described by Zheng *et al*.[51] Fmoc-Thr(tBu)-OH was manually coupled onto the hydrazine and a loading test was carried out, finding a loading of 0.3 mmol/g. The peptide was then further synthesized using the general automated SPPS conditions, using the formic acid containing Fmoc deprotection solution (1:20:79 CHOOH/piperidine/DMF). The $Val_{80}Thr_{81}$ dipeptide was incorporated as the Fmoc-Val-Thr(ψ(Me,Me)pro)-OH pseudoproline dipeptide building block. Global deprotection followed by RP-HPLC purification yielded compound **12** as a white solid (14.2 mg, 3.5 µmol, 7.7%). **LC-MS** RT = 3.7 min (C18, 10-50% B over 9 minutes) **LRMS** calcd $[M+3H]^{3+}$ = 1366.7, $[M+4H]^{4+}$ = 1025.3 observed M/z = 1367.2, 1025.8

Cys-Phe-Phe-Arg-Asp-His-Ser-Tyr-Gln-Glu-Glu-Ala-Ala-Met-Glu-Leu-Lys-Val-Glu-Asp-Pro-Phe-Tyr-Trp-Val-Ser-Pro-Gly-OH (14)

The peptide was synthesized using the standard methods for automated peptide synthesis starting from glycine preloaded Tentagel S Ac. Global deprotection followed by RP-HPLC purification yielded compound **14** as a white solid (4.9 mg, 1.5 µmol, 1.4%) **LC-MS** RT = 16.8 min (C18, 5-65% B over 30 minutes) **LRMS** calcd $[M+3H]^{3+}$ = 1127.8 observed M/z = 1128.1

Val-His-Leu-Tyr-Arg-Asn-NH_2 (20)

Synthesized on Tentagel S RAM resin (50 µmol) using the standard conditions for manual SPPS. Global deprotection followed by RP-HPLC purification yielded compound **20** as a white solid (26.5 mg, 33.2 µmol, 66%). **LC-MS** RT = 3.7 min (C18, 10-90% B over 9 minutes) **LRMS** calcd $[M+H]^{+}$ = 800.45 observed M/z = 800.53

General procedure for the on-resin synthesis of OCam peptide esters

The OCam function is introduced onto the resin by coupling 2 equivalents of Fmoc-OCH_2COOH, activated with 2 equivalents of HCTU (as 0.2 M in DMF) and 4 equivalents of DiPEA for 90 minutes. After Fmoc removal following the standard protocols, the C-terminal amino acid is acylated onto the alcohol using 4 equivalents of Fmoc-amino acid, together with 6 equivalents of DIC and 0.4 equivalents of DMAP. This reaction was allowed to proceed for 45 minutes. For sterically hindered amino acids, the procedure is repeated once. The Fmoc group is then removed by treatment with 20 % (v/v) piperidine for 2 minutes, repeated once, in order to limit aminolysis. The following amino acid is then coupled as normal. In order to limit diketopiperazine formation, the next Fmoc group was removed using 2% (v/v) DBU in DMF for 10 minutes. This free amine was, after thorough washing (5 x DMF) immediately coupled with the next amino acid using standard protocols. From this point on, the synthesis of the peptide was carried out as normal using either manual or automated Fmoc-SPPS protocols.

Pro-Phe-Ser-Arg-Val-OCam-Leu-NH_2 (18)

Peptide was synthesized on Tentagel S RAM resin (50 µmol) using the procedures for introduction of OCam esters followed by manual synthesis. Global deprotection followed by RP-HPLC purification yielded compound **18** as a white solid (24,8 mg, 32.0 µmol, 64%) **LC-MS** RT = 5.3 min (C18, 10-50% B over 9 minutes) **LRMS** calcd $[M+H]^+$ = 775.44 observed M/z = 775.60

Pro-Phe-Ser-Cit-Val-OCam-Leu-NH_2 (19)

Peptide was synthesized on Tentagel S RAM resin (50 µmol) using the procedures for introduction of OCam esters followed by manual synthesis. Global deprotection followed by RP-HPLC purification yielded compound **19** as a white solid (22,7 mg, 29.3 µmol, 59%). **LC-MS** RT = 5.5 min (C18, 10-50% B over 9 minutes) **LRMS** calcd $[M+2H]^{2+}$ = 776.42 observed M/z = 776.60

Pro-Gly-Lys-Asn-Ala-Thr-Gly-Met-Glu-Val-Gly-Trp-Tyr-Arg-Pro-Pro-Phe-Ser-Arg-Val-OCam-Leu-Lys-Lys-NH_2 (23)

Peptide was synthesized on Tentagel S RAM resin (100 µmol) using the procedures for introduction of OCam esters followed by manual synthesis. Global deprotection followed by RP-HPLC purification yielded compound **23** as a white solid (80.7 mg, 30.2 µmol, 30%) **LC-MS** RT = 5.2 min (C18, 10-90% B over 9 minutes) **LRMS** calcd $[M+3H]^{3+}$ = 892.81 observed M/z = 893.17

Ac-Gly-Gln-Phe-Arg-Val-Ile-Gly-Pro-Arg-His-Pro-Ile-Arg-Ala-Leu-Val-Gly-Asp-Glu-Val-Glu-Leu-Pro-Cys-Arg-Ile-Ser-Pro-Gly-Lys-Asn-Ala-Thr-Gly-Met-Glu-Val-Gly-Trp-Tyr-Arg-Pro-Pro-Phe-Ser-Arg-Val-OCam-Leu-Lys-Lys-NH_2 (26)

Peptide was synthesized on Tentagel S RAM resin (100 µmol) using the procedures for introduction of OCam esters followed by automated synthesis. After Fmoc deprotection, the N-terminus was acetylated using 10% (v/v) Ac_2O and 5% (v/v) DiPEA in DMF for 15 minutes. Global deprotection followed by RP-HPLC purification yielded compound **26** as a white solid (42.2 mg, 7.4 µmol, 7%) **LC-MS** RT = 14.9 min (C18, 5-65% B over 30 minutes) **LRMS** calcd $[M+4H]^{4+}$ = 1429.52 observed M/z = 1429.83

Recombinant expression of His-tagged MOG-fragments

Expression and purification of His-tagged MOG fragments was carried out as described by Araman *et al.*[2] with a few minor changes: For the MOG_{49-125}-TEV-His_6 fragment, four different solubilization buffers were tested: 6 M Gdn·HCl, 200 mM NaPi, 300 mM NaCl, pH 8; 6 M Urea, 200 mM NaPi, 300 mM NaCl, pH 8; 6 M Urea, 200 mM Tricine, 300 mM NaCl, pH 8; 8 M Urea, 200 mM Tricine, 300 mM NaCl, pH 8.5; Desalting buffers with the same compositions (minus the NaCl) were used in tandem.

General protocol for NCL

Ligation buffer (6 M Gdn·HCl, 200 mM NaPi, pH 7.2) was degassed with N2 for 30 minutes prior to use. TCEP·HCl and the desired thiol catalyst (MPAA or TFET) were dissolved in this buffer, pH adjusted to the desired value, and the resulting solution was again degassed with N2. Then, the thioester fragment (1.0 eq, 2 mM) and cysteine fragment (1.5 eq., 3 mM) are dissolved in 100 µL of this mixture. The ligation mixture was shaken at 600 rpm at the specified temperature. Fresh TCEP (as 100 mM solution in ligation buffer) was added after 4 and 24. Time points (0, 1,2,4,24 and (for proline ligation) 48 hours) were taken as aliquots of 10 µl, acidified with 10µl 20% (v/v) aqueous TFA and stored at -80°C. The aliquot was diluted with 30 µl buffer prior to LC-MS analysis.

Omniligase-1 ligation of Arg and Cit containing model peptides

The peptide ester and the amine fragments were prepared as 10 mM stock solutions in ligation buffer (200 mM tricine, pH 8.5). From these, a reaction mixture was made containing 1 mM of both peptides and 6 mM TCEP, in a total volume of 200 µL ligation buffer. The pH was calibrated to be 8.5 and Omniligase-1 was added (1 µL of a 5 mg/mL stock). Samples were taken at 0, 1 2 and 4 hours by diluting 10 µL of ligation mixture in 90 µL of quenching solution (2:9:9 TFA:MeCN:H_2O). These samples were analyzed by LC-MS.

Omniligase-1 ligation onto $MOG_{49\text{-}125}$-TEV-His_6

Reduction of chaotrope concentration in protein solution was carried out as follows: 500 µL of protein solution was applied to an Amicon Ultra-0.5 Centrifugal Filter (3 kDa NMWCO), which was spun at the manufacturers recommended speed (14000 rcf) and 8°C until half of the solution had run through the filter. Then, the sample was diluted with chaotrope-free buffer to achieve the desired chaotrope concentration. When necessary, this procedure was repeated.

Peptide ester (5 or 10 equivalents, based on protein concentration) was dissolved in 100 µL of protein solution in denaturing buffer. TCEP was added from a 100 mg/mL solution to make the final TCEP concentration 6 mM (1.5 µL). The pH was set to 8.5 and Omniligase-1 was added from a 5 mg/mL stock solution. LC-MS samples were taken at 0, 1 2 and 4 hours by diluting 10 µL of ligation mixture in 90 µL of quenching solution (2:9:9 TFA:MeCN:H_2O). Additional samples for SDS-PAGE analysis were taken by diluting 2.5 µL of reaction mixture with 12.5 µL denaturing buffer (8 M Urea, 200 mM tricine, pH 8.5), followed by an equal volume (15 µL) loading buffer (Laemmli).

Carboxyamidometyl-ester stability tests

1 µmol of resin-bound peptide **27** (Fmoc-Ser(tBu)-Arg(Pbf)-Val-OCam-Leu-Lys(Boc)-Lys(Boc)-RAM) was added into a vial and 500 µL of the deprotection solution under investigation was added. The vial was screwed close and put in a heating block, were it was stirred for 4 hours at the indicated temperatures (RT, 50°C or 90°C). After the four hours had elapsed, the vials were cooled back to room temperature and the resin was transferred to a fritted syringe and thoroughly washed with DMF. Next, the resin was treated with 0.5 mL capping solution containing 0.5 M Bz_2O, 0.5 M DiPEA and 0.1 M pyridine in DMF for 30 minutes. After capping, the peptides were cleaved from resin (95:2.5:2.5 TFA/H_2O/TIS, 200 µL, 1 hour), precipitated from cold Et_2O and recovered by centrifugation. The pellets were dissolved in 1 mL of 1:1:1 MeCN/tBuOH/H_2O and subjected to LC-MS analysis.

Experimental for $OVA_{323\text{-}339}$ glycocluster-scaffold-peptides

General procedure for peptides synthesis

All solid support peptide synthesis, including selective Mmt deprotection and fluorophore incorporation, was carried out as described in Chapter 4.

Fmoc-Lys(N_3)-Lys(N_3)-Lys(N_3)-Lys(N_3)-Lys(N_3)-Lys(N_3)-Gly-Ile-Ser(tBu)-Gln(Trt)-Ala-Val-His(Boc)-Ala-Ala-His(Boc)-Ala-Glu(OtBu)-Ile-Asn(Trt)-Glu(OtBu)-Ala-Gly-Arg(Pbf)-Ala-Ala-Ala-Ala-Ala-Lys(Mmt)-RAM-Tentagel S (29)

The synthesis was carried out on Tentagel S RAM resin (25 µmol) using a combination of manual and automatic SPPS conditions. **LC-MS** RT = 7.7 min (C18, 10-90% B over 9 minutes) **LRMS** calcd $[M+2H]^{2+}$ = 1730.90, $[M+3H]^{3+}$ = 1154.26 observed M/z = 1730.80, 1154.60

Lys(N_3)-Lys(N_3)-Lys(N_3)-Lys(N_3)-Lys(N_3)-Lys(N_3)-Gly-Ile-Ser-Gln-Ala-Val-His-Ala-Ala-His-Ala-Glu-Ile-Asn-Glu-Ala-Gly-Arg-Ala-Ala-Ala-Ala-Ala-Lys(sCy5)-RAM-Tentagel S (30)

Immobilized peptide **29** (5 µmol) was selectively deprotected followed by incorporation of the sCy5 fluorophore, according to the general methods. The Fmoc-group was then removed using standard conditions and the peptide liberated from resin. **LC-MS** RT = 5.0 min (C18, 10-90% B over 9 minutes) **LRMS** calcd $[M+2H]^{2+}$ = 1931.96, $[M+3H]^{3+}$ = 1288.31 observed M/z = 1921.25, 1288.50

Lys(N_3)-Lys(N_3)-Lys(N_3)-Lys(N_3)-Lys(N_3)-Lys(N_3)-Gly-Ile-Ser-Gln-Ala-Val-His-Ala-Ala-His-Ala-Glu-Ile-Asn-Glu-Ala-Gly-Arg-Ala-Ala-Ala-Ala-Ala-Lys(sCy5)-RAM-Tentagel S (31)

Immobilized peptide **29** (5 µmol) was N-terminally acetylated following the general protocol. The Mmt group was then selectively deprotected, followed by incorporation of the sCy5 fluorophore, according to the general methods. Finally, the peptide was liberated from resin. **LC-MS** RT = 6.0 min (C18, 10-90% B over 9 minutes) **LRMS** calcd $[M+2H]^{2+}$ = 1953.97, $[M+3H]^{3+}$ = 1302.31 observed M/z = 1953.50, 1302.50

Experimental for cyclic scaffolds

General procedure for peptides synthesis

All solid support peptide synthesis, including head-to-tail cyclization and selective Mmt deprotection, was carried out as described in Chapter 5.

***Cyclo*(-Lys-Abu-Lys(TEG-N_3)-Abu-Lys(TEG-N_3)-Abu-Lys(TEG-N_3)-Abu-Lys(TEG-N_3)-Abu-) (43)**

Peptide synthesis was initiated on a 25 µmol scale. Following the general procedures for cyclization and sidechain modification, compound **43** was isolated using RP-HPLC in 9.8% (4.6 mg, 2.4 µmol) yield. **LC-MS** RT = 5.2 min (C18, 10-90% B over 9 minutes) **LRMS** calcd $[M+H]^{+}$ = 1927.1, $[M+2H]^{2+}$ = 964.10; observed M/z = 1926.87,964.07

***Cyclo*(-Lys-Abu-Lys(TEG-TEG-N_3)-Abu-Lys(TEG-TEG-N_3)-Abu-Lys(TEG-TEG-N_3)-Abu-Lys(TEG-TEG-N_3)-Abu-) (44)**

Peptide synthesis was initiated on a 25 µmol scale. Following the general procedures for cyclization and sidechain modification, compound **44** was isolated using RP-HPLC in 4.5% (3.0 mg, 1.1 µmol) yield. **LC-MS** RT = 4.4 min (C18, 10-90% B over 9 minutes) **LRMS** calcd $[M+2H]^{2+}$ = 1342.75, $[M+3H]^{3+}$ = 895.5; observed M/z = 1342.83, 895.58

Biophysical, biochemical and computational assays

ThT Fluorescence Aggregation Assays

Aggregation assays were carried out in 96-well plate format using a Infinite M1000 Pro Tecan plate reader. The excitation and emission wavelengths were set to 444 nm and 485 nm respectively, with a

bandwidth of 10 nm. For each peptide under investigation, a 200 µM stock in sodium ascorbate buffer (20 mM, pH=5) was prepared and from this stock a serial diluted was made using the same buffer. Of these solutions, 199 µL of peptide stock was added into a well and mixed with 1 µL of 1 mM Thioflavin T stock solution, prepared in the same NaOAc buffer, for a final dye concentration of 5 µM. Every concentration of peptide was measured in triplicate. The plate was kept at 37°C and the fluorescence was measured every ten minutes for 16 hours. The fluorescence was normalized against a well containing 5 µM Thioflavin T in buffer that was measured alongside the assay.

Molecular Docking

The structures of HLA-E were retrieved from the Protein Data Bank using ICM Molsoft's inbuilt feature. The two entries with a resolution < 2.5 Å were visually inspected and 6GH1 was selected for its slightly better resolution. Of this structure chain A and peptide P were converted to an ICM object, with 'optimize hydrogens' set to true. 'Tight' water molecules were retained, leading to a conserved water molecule being present in the binding cleft near the peptides N-terminus. This water molecule is present in around half of the structures in the PDB. The bound 9-mer epitope was isolated to a separate object and used as template to select the binding cleft by selecting all atoms of the protein in a 5.0 Å radius. A pocket box was defined around this selection using default settings. The MOG_{40-48} epitopes of human (YRPPFSRVV) and mouse (YRSPFSRVV) and their 46-Citr variants were loaded from an SD-file and docked with the 'thoroughness' parameter set to 10, the 10 best poses were retained. The resulting poses were manually inspected and visualised using the Open Source PyMOL application.

Cathepsin G degradation assay

Peptides (10 µM) were dissolved in 200 µL sodium acetate buffer (150 mM, pH 5) and 50 ng of human cathepsin G (Abcam, ab91122) was added as 0.5 µL of a 0.1 mg/mL stock solution in NaOAc buffer (150 mM NaOAc, 150 mM NaCl, pH 5.5). The enzymatic reactions were incubated at 37°C and gently mixed at 600 RPM using an Eppendorf® ThermoMixer® C equipped with an Eppendorf® SmartBlock® for 1.5 mL epps. At specific timepoints (0, 1, 2, 4 and 24 hours) a 20 µL sample was taken. This sample was diluted with a quenching buffer (20 µL, 45:45:10 H_2O/MeCN/TFA) containing 100 µM Cbz-Phe-OH as an internal standard. These samples were analysed on a Thermo Scientific Vanquish UHPLC coupled to a Thermo Scientific LCQ Fleet ion mass spectrometer using a gradient of 5-65% B with constant 10% C over 30 minutes (buffer A: H_2O; buffer B: MeCN; buffer C: 1% TFA in H_2O). The peak at RT = 20.4 minutes was determined to belong to the internal standard and the ratio of the area under this peak to the area under the starting peptide peak was determined for all time points, using 220 nm as the absorption wavelength. The peak area ratio at t = 0 was set to 100%. Newly produced fragments were assigned to peptide sequences by analysis of the ESI+ mass spectrum.

Supporting Figures

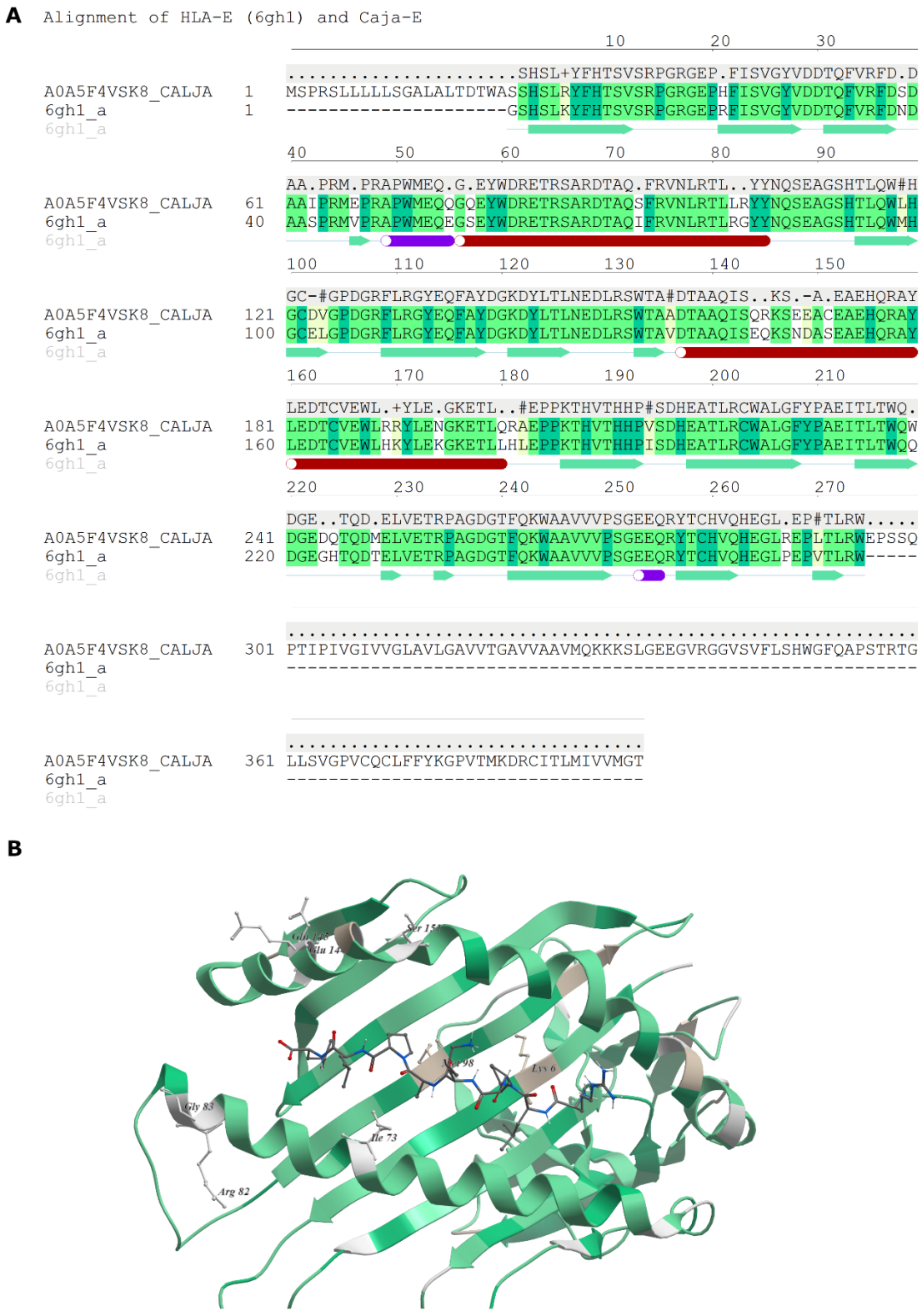

Figure S1. A) Alignment of amino acid sequence between HLA-E (PDB 6gh1, 6gh1_a) and Caja-E (A0A5F4VSK8_CALJA) B) HLA-E crystal structure (PDB 6gh1) showing the peptide binding groove. All residues not identical to those in Caja-E are highlighted in gray. Image generated by A.P.A. Janssen (Leiden university).

Table S1. Overview of ligation conditions tested on MOG27-47-OCamLKK (**23**) with MOG48-125-TEV-His_6 (**24**).

#	Buffer composition	Enzyme (µg/mL)	[Protein fragment] (µM)	Peptide (eq.)	Remarks
1	2 M guanidine 200 mM phosphate	500	360	5	low conversion (~20%), precipitated
2	2 M guanidine 200 mM phosphate	500	360	10	moderate conversion (~50%), precipitated
3	1.5 M guanidine 200 mM phosphate	500	250	5	low conversion (~20%), precipitated
4	1.5 M guanidine 200 mM phosphate	500	250	10	moderate conversion (~50%), precipitated
5	1 M guanidine 200 mM phosphate	500	180	5	very low conversion (<10%), precipitated
6	1 M guanidine 200 mM phosphate	500	180	10	low conversion (~20%), precipitated
7	6 M urea 200 mM tricine	250	190	10	moderate conversion (~40%)
8	6 M urea 200 mM phosphate	250	230	10	moderate conversion (~40%)
9	4 M urea 200 mM tricine	250	235	10	moderate conversion (~40%)
10	4 M urea 200 mM phosphate	250	185	10	moderate conversion (~40%)
11	4 M urea 200 mM tricine	50	235	10	moderate conversion (~40%)
12	4 M urea 200 mM phosphate	50	185	10	moderate conversion (~40%)
13	2 M urea 200 mM tricine	50	170	10	moderate conversion (~40%), precipitated
14	2 M urea 200 mM phosphate	50	200	10	moderate conversion (~40%), precipitated

References

(1) Doelman, W.; Marqvorsen, M. H. S.; Chiodo, F.; Bruijns, S. C. M.; van der Marel, G. A.; van Kooyk, Y.; van Kasteren, S. I.; Araman, C. Synthesis of Asparagine Derivatives Harboring a Lewis X Type DC-SIGN Ligand and Evaluation of Their Impact on Immunomodulation in Multiple Sclerosis. *Chem. Eur. J.* **2021**, *27* (8), 2742–2752. https://doi.org/10.1002/chem.202004076.

(2) Araman, C.; van Gent, M. E.; Meeuwenoord, N. J.; Heijmans, N.; Marqvorsen, M. H. S.; Doelman, W.; Faber, B. W.; 't Hart, B. A.; Van Kasteren, S. I. Amyloid-like Behavior of Site-Specifically Citrullinated Myelin Oligodendrocyte Protein (MOG) Peptide Fragments inside EBV-Infected B-Cells Influences Their Cytotoxicity and Autoimmunogenicity. *Biochemistry* **2019**, *58* (6), 763–775. https://doi.org/10.1021/acs.biochem.8b00852.

(3) Riera, R.; Hogervorst, T. P.; Doelman, W.; Ni, Y.; Pujals, S.; Bolli, E.; Codée, J. D. C.; van Kasteren, S. I.; Albertazzi, L. Single-Molecule Imaging of Glycan–Lectin Interactions on Cells with Glyco-PAINT. *Nat. Chem. Biol.* **2021**, *17* (12), 1281–1288. https://doi.org/10.1038/s41589-021-00896-2.

(4) Li, R. J. E.; Hogervorst, T. P.; Achilli, S.; Bruijns, S. C.; Arnoldus, T.; Vivès, C.; Wong, C. C.; Thépaut, M.; Meeuwenoord, N. J.; van den Elst, H.; Overkleeft, H. S.; van der Marel, G. A.; Filippov, D. V.; van Vliet, S. J.; Fieschi, F.; Codée, J. D. C.; van Kooyk, Y. Systematic Dual Targeting of Dendritic Cell C-Type Lectin Receptor DC-SIGN and TLR7 Using a Trifunctional Mannosylated Antigen. *Front. Chem.* **2019**, *7*, 650. https://doi.org/10.3389/fchem.2019.00650.

(5) van der Gracht, A. M. F.; de Geus, M. A. R.; Camps, M. G. M.; Ruckwardt, T. J.; Sarris, A. J. C.; Bremmers, J.; Maurits, E.; Pawlak, J. B.; Posthoorn, M. M.; Bonger, K. M.; Filippov, D. V; Overkleeft, H. S.; Robillard, M. S.; Ossendorp, F.; van Kasteren, S. I. Chemical Control over T-Cell Activation in Vivo Using Deprotection of Trans -Cyclooctene-Modified Epitopes. *ACS Chem. Biol.* **2018**, *13* (6), 1569–1576. https://doi.org/10.1021/acschembio.8b00155.

(6) Fairbanks, A. J. The ENGases: Versatile Biocatalysts for the Production of Homogeneous N-Linked Glycopeptides and Glycoproteins. *Chem. Soc. Rev.* **2017**, *46* (16), 5128–5146. https://doi.org/10.1039/C6CS00897F.

(7) Fujita, M.; Shoda, S. ichiro; Haneda, K.; Inazu, T.; Takegawa, K.; Yamamoto, K. A Novel Disaccharide Substrate Having 1,2-Oxazoline Moiety for Detection of Transglycosylating Activity of Endoglycosidases. *Biochim. Biophys. Acta - Gen. Subj.* **2001**, *1528* (1), 9–14. https://doi.org/10.1016/S0304-4165(01)00164-7.

(8) McIntosh, J. D.; Brimble, M. A.; Brooks, A. E. S.; Dunbar, P. R.; Kowalczyk, R.; Tomabechi, Y.; Fairbanks, A. J. Convergent Chemo-Enzymatic Synthesis of Mannosylated Glycopeptides; Targeting of Putative Vaccine Candidates to Antigen Presenting Cells. *Chem. Sci.* **2015**, *6* (8), 4636–4642. https://doi.org/10.1039/c5sc00952a.

(9) Bosques, C. J.; Imperiali, B. The Interplay of Glycosylation and Disulfide Formation Influences Fibrillization in a Prion Protein Fragment. *Proc. Natl. Acad. Sci.* **2003**, *100* (13), 7593–7598. https://doi.org/10.1073/pnas.1232504100.

(10) Liu, C. P.; Tsai, T. I.; Cheng, T.; Shivatare, V. S.; Wu, C. Y.; Wu, C. Y.; Wong, C. H. Glycoengineering of Antibody (Herceptin) through Yeast Expression and in Vitro Enzymatic Glycosylation. *Proc. Natl. Acad. Sci. U. S. A.* **2018**, *115* (4), 720–725. https://doi.org/10.1073/pnas.1718172115.

(11) Jagessar, S. A.; Kap, Y. S.; Heijmans, N.; Van Driel, N.; Van Straalen, L.; Bajramovic, J. J.; Brok, H. P. M.; Blezer, E. L. A.; Bauer, J.; Laman, J. D.; 'T Hart, B. A. Induction of Progressive Demyelinating Autoimmune Encephalomyelitis in Common Marmoset Monkeys Using MOG34-56 Peptide in Incomplete Freund Adjuvant. *J. Neuropathol. Exp. Neurol.* **2010**, *69* (4), 372–385. https://doi.org/10.1097/NEN.0b013e3181d5d053.

(12) Embgenbroich, M.; Burgdorf, S. Current Concepts of Antigen Cross-Presentation. *Front. Immunol.* **2018**, *0* (JUL), 1643. https://doi.org/10.3389/FIMMU.2018.01643.

(13) Jagessar, S. A.; Heijmans, N.; Blezer, E. L. A.; Bauer, J.; Blokhuis, J. H.; Wubben, J. A. M.; Drijfhout, J. W.; van den Elsen, P. J.; Laman, J. D.; Hart, B. A. '. Unravelling the T-Cell-Mediated Autoimmune Attack on CNS Myelin in a New Primate EAE Model Induced with MOG 34-56 Peptide in Incomplete Adjuvant. *Eur. J. Immunol.* **2012**, *42* (1), 217–227. https://doi.org/10.1002/eji.201141863.

(14) Jagessar, S. A.; Holtman, I. R.; Hofman, S.; Morandi, E.; Heijmans, N.; Laman, J. D.; Gran, B.; Faber, B. W.; van Kasteren, S. I.; Eggen, B. J. L.; 't Hart, B. A. Lymphocryptovirus Infection of Nonhuman Primate B Cells Converts Destructive into Productive Processing of the Pathogenic CD8 T Cell Epitope in Myelin Oligodendrocyte Glycoprotein. *J. Immunol.* **2016**, *197* (4), 1074–1088. https://doi.org/10.4049/jimmunol.1600124.

(15) Morandi, E.; Jagessar, S. A.; 't Hart, B. A.; Gran, B. EBV Infection Empowers Human B Cells for Autoimmunity: Role of Autophagy and Relevance to Multiple Sclerosis. *J. Immunol.* **2017**, *199* (2), 435–448.

(16) Burster, T.; Beck, A.; Tolosa, E.; Marin-Esteban, V.; Rötzschke, O.; Falk, K.; Lautwein, A.; Reich, M.; Brandenburg, J.; Schwarz, G.; Wiendl, H.; Melms, A.; Lehmann, R.; Stevanovic, S.; Kalbacher, H.; Driessen, C. Cathepsin G, and Not the Asparagine-Specific Endoprotease, Controls the Processing of Myelin Basic Protein in Lysosomes from Human B Lymphocytes. *J. Immunol.* **2004**, *172* (9), 5495–5503. https://doi.org/10.4049/JIMMUNOL.172.9.5495.

(17) Carrillo-Vico, A.; Leech, M. D.; Anderton, S. M. Contribution of Myelin Autoantigen Citrullination to T Cell Autoaggression in the Central Nervous System. *J. Immunol.* **2010**, *184* (6), 2839–2846. https://doi.org/10.4049/jimmunol.0903639.

(18) Van Leeuwen, T.; Araman, C.; Pieper Pournara, L.; Kampstra, A. S. B.; Bakkum, T.; Marqvorsen, M. H. S.; Nascimento, C. R.; Groenewold, G. J. M.; Van Der Wulp, W.; Camps, M. G. M.; Janssen, G. M. C.; Van Veelen, P. A.; Van Westen, G. J. P.; Janssen, A. P. A.; Florea, B. I.; Overkleeft, H. S.; Ossendorp, F. A.; Toes, R. E. M.; Van Kasteren, S. I. Bioorthogonal Protein Labelling Enables the Study of Antigen Processing of Citrullinated and Carbamylated Auto-Antigens. *RSC Chem. Biol.* **2021**, *2* (3), 855–862. https://doi.org/10.1039/D1CB00009H.

(19) Thorpe, M.; Fu, Z.; Chahal, G.; Akula, S.; Kervinen, J.; De Garavilla, L.; Hellman, L. Extended Cleavage Specificity of Human Neutrophil Cathepsin G: A Low Activity Protease with Dual Chymase and Tryptase-Type Specificities. *PLoS One* **2018**, *13* (4), e0195077. https://doi.org/10.1371/JOURNAL.PONE.0195077.

(20) Dawson, P. E.; Muir, T. W.; Clark-Lewis, I.; Kent, S. B. H. Synthesis of Proteins by Native Chemical Ligation. *Science* **1994**, *266* (5186), 776–779. https://doi.org/10.1126/science.7973629.

(21) Agouridas, V.; El Mahdi, O.; Diemer, V.; Cargoët, M.; Monbaliu, J. C. M.; Melnyk, O. Native Chemical Ligation and Extended Methods: Mechanisms, Catalysis, Scope, and Limitations. *Chemical Reviews*. American Chemical Society June 26, 2019. https://doi.org/10.1021/acs.chemrev.8b00712.

(22) Miseta, A.; Csutora, P. Relationship Between the Occurrence of Cysteine in Proteins and the Complexity of Organisms. *Mol. Biol. Evol.* **2000**, *17* (8), 1232–1239. https://doi.org/10.1093/OXFORDJOURNALS.MOLBEV.A026406.

(23) Carugo, O. Amino Acid Composition and Protein Dimension. *Protein Sci.* **2008**, *17* (12), 2187–2191. https://doi.org/10.1110/PS.037762.108.

(24) Yan, L. Z.; Dawson, P. E. Synthesis of Peptides and Proteins without Cysteine Residues by Native Chemical Ligation Combined with Desulfurization. *J. Am. Chem. Soc.* **2001**, *123* (4), 526–533.

https://doi.org/10.1021/ja003265m.

(25) Wan, Q.; Danishefsky, S. J. Free-Radical-Based, Specific Desulfurization of Cysteine: A Powerful Advance in the Synthesis of Polypeptides and Glycopolypeptides. *Angew. Chem. Int. Ed.* **2007**, *46* (48), 9248–9252. https://doi.org/10.1002/ANIE.200704195.

(26) Hackeng, T. M.; Griffin, J. H.; Dawson, P. E. Protein Synthesis by Native Chemical Ligation: Expanded Scope by Using Straightforward Methodology. *Proc. Natl. Acad. Sci.* **1999**, *96* (18), 10068–10073. https://doi.org/10.1073/PNAS.96.18.10068.

(27) Camarero, J.; Mitchell, A. Synthesis of Proteins by Native Chemical Ligation Using Fmoc-Based Chemistry. *Protein Pept. Lett.* **2005**, *12* (8), 723–728. https://doi.org/10.2174/0929866054864166.

(28) Ollivier, N.; Dheur, J.; Mhidia, R.; Blanpain, A.; Melnyk, O. Bis(2-Sulfanylethyl)Amino Native Peptide Ligation. *Org. Lett.* **2010**, *12* (22), 5238–5241. https://doi.org/10.1021/ol102273u.

(29) Blanco-Canosa, J. B.; Dawson, P. E. An Efficient Fmoc-SPPS Approach for the Generation of Thioester Peptide Precursors for Use in Native Chemical Ligation. *Angew. Chem. Int. Ed.* **2008**, *47* (36), 6851–6855. https://doi.org/10.1002/ANIE.200705471.

(30) Yang, Y.; Sweeney, W. V.; Schneider, K.; Thörnqvist, S.; Chait, B. T.; Tam, J. P. Aspartimide Formation in Base-Driven 9-Fluorenylmethoxycarbonyl Chemistry. *Tetrahedron Lett.* **1994**, *35* (52), 9689–9692. https://doi.org/10.1016/0040-4039(94)88360-2.

(31) Cardona, V.; Eberle, I.; Barthélémy, S.; Beythien, J.; Doerner, B.; Schneeberger, P.; Keyte, J.; White, P. D. Application of Dmb-Dipeptides in the Fmoc SPPS of Difficult and Aspartimide-Prone Sequences. In *International Journal of Peptide Research and Therapeutics*; Springer, 2008; Vol. 14, pp 285–292. https://doi.org/10.1007/s10989-008-9154-z.

(32) Michels, T.; Dölling, R.; Haberkorn, U.; Mier, W. Acid-Mediated Prevention of Aspartimide Formation in Solid Phase Peptide Synthesis. *Org. Lett.* **2012**, *14* (20), 5218–5221. https://doi.org/10.1021/ol3007925.

(33) Blanco-Canosa, J. B.; Nardone, B.; Albericio, F.; Dawson, P. E. Chemical Protein Synthesis Using a Second-Generation N-Acylurea Linker for the Preparation of Peptide-Thioester Precursors. *J. Am. Chem. Soc.* **2015**, *137* (22), 7197–7209. https://doi.org/10.1021/jacs.5b03504.

(34) Clements, C. S.; Reid, H. H.; Beddoe, T.; Tynan, F. E.; Perugini, M. A.; Johns, T. G.; Bernard, C. C. A.; Rossjohn, J. The Crystal Structure of Myelin Oligodendrocyte Glycoprotein, a Key Autoantigen in Multiple Sclerosis. *Proc. Natl. Acad. Sci.* **2003**, *100* (19), 11059–11064. https://doi.org/10.1073/PNAS.1833158100.

(35) White, P.; Keyte, J. W.; Bailey, K.; Bloomberg, G. Expediting the Fmoc Solid Phase Synthesis of Long Peptides through the Application of Dimethyloxazolidine Dipeptides. *J. Pept. Sci.* **2004**, *10* (1), 18–26. https://doi.org/10.1002/PSC.484.

(36) El Oualid, F.; Merkx, R.; Ekkebus, R.; Hameed, D. S.; Smit, J. J.; de Jong, A.; Hilkmann, H.; Sixma, T. K.; Ovaa, H.; El Oualid, F.; Merkx, R.; Ekkebus, R.; Hameed, D. S.; de Jong, A.; Hilkmann, H.; Ovaa, H.; Smit, J. J.; Sixma, T. K. Chemical Synthesis of Ubiquitin, Ubiquitin-Based Probes, and Diubiquitin. *Angew. Chem. Int. Ed.* **2010**, *49* (52), 10149–10153. https://doi.org/10.1002/ANIE.201005995.

(37) Fang, G. M.; Li, Y. M.; Shen, F.; Huang, Y. C.; Li, J. Bin; Lin, Y.; Cui, H. K.; Liu, L. Protein Chemical Synthesis by Ligation of Peptide Hydrazides. *Angew. Chem. Int. Ed.* **2011**, *50* (33), 7645–7649. https://doi.org/10.1002/ANIE.201100996.

(38) Jin, K.; Li, X. Advances in Native Chemical Ligation–Desulfurization: A Powerful Strategy for Peptide and Protein Synthesis. *Chem. – A Eur. J.* **2018**, *24* (66), 17397–17404.

https://doi.org/10.1002/CHEM.201802067.

(39) Thompson, R. E.; Liu, X.; Alonso-García, N.; Pereira, P. J. B.; Jolliffe, K. A.; Payne, R. J. Trifluoroethanethiol: An Additive for Efficient One-Pot Peptide Ligation - Desulfurization Chemistry. *J. Am. Chem. Soc.* **2014**, *136* (23), 8161–8164. https://doi.org/10.1021/ja502806r.

(40) Schmidt, M.; Toplak, A.; Quaedflieg, P. J. L. M.; Ippel, H.; Richelle, G. J. J.; Hackeng, T. M.; van Maarseveen, J. H.; Nuijens, T. Omniligase-1: A Powerful Tool for Peptide Head-to-Tail Cyclization. *Adv. Synth. Catal.* **2017**, *359* (12), 2050–2055. https://doi.org/10.1002/ADSC.201700314.

(41) Nuijens, T.; Toplak, A.; Schmidt, M.; Ricci, A.; Cabri, W. Natural Occurring and Engineered Enzymes for Peptide Ligation and Cyclization. *Front. Chem.* **2019**, *7*, 829. https://doi.org/10.3389/fchem.2019.00829.

(42) Pawlas, J.; Nuijens, T.; Persson, J.; Svensson, T.; Schmidt, M.; Toplak, A.; Nilsson, M.; Rasmussen, J. H. Sustainable, Cost-Efficient Manufacturing of Therapeutic Peptides Using Chemo-Enzymatic Peptide Synthesis (CEPS). *Green Chem.* **2019**, *21* (23), 6451–6467. https://doi.org/10.1039/C9GC03600H.

(43) Schmidt, M.; Nuijens, T. Chemoenzymatic Synthesis of Linear- and Head-to-Tail Cyclic Peptides Using Omniligase-1. In *Enzyme-Mediated Ligation Methods*; Nuijens, T., Schmidt, M., Eds.; Springer New York: New York, NY, 2019; pp 43–61. https://doi.org/10.1007/978-1-4939-9546-2_4.

(44) Nuijens, T.; Toplak, A.; van de Meulenreek, M. B. A. C.; Schmidt, M.; Goldbach, M.; Quaedflieg, P. J. L. M. Improved Solid Phase Synthesis of Peptide Carboxyamidomethyl (Cam) Esters for Enzymatic Segment Condensation. *Tetrahedron Lett.* **2016**, *57* (32), 3635–3638. https://doi.org/10.1016/J.TETLET.2016.06.132.

(45) Burgdorf, S.; Kautz, A.; Böhnert, V.; Knolle, P. A.; Kurts, C. Distinct Pathways of Antigen Uptake and Intracellular Routing in CD4 and CD8 T Cell Activation. *Science* **2007**, *316* (5824), 612–616. https://doi.org/10.1126/science.1137971.

(46) Mitchell, D. A.; Fadden, A. J.; Drickamer, K. A Novel Mechanism of Carbohydrate Recognition by the C-Type Lectins DC-SIGN and DC-SIGNR. Subunit Organization and Binding to Multivalent Ligands. *J. Biol. Chem.* **2001**, *276* (31), 28939–28945. https://doi.org/10.1074/jbc.M104565200.

(47) Ghosh, P.; Dahms, N. M.; Kornfeld, S. Mannose 6-Phosphate Receptors: New Twists in the Tale. *Nat. Rev. Mol. Cell Biol. 2003 43* **2003**, *4* (3), 202–213. https://doi.org/10.1038/nrm1050.

(48) Reintjens, N. R. M. M.; Tondini, E.; Vis, C.; McGlinn, T.; Meeuwenoord, N. J.; Hogervorst, T. P.; Overkleeft, H. S.; Filippov, D. V.; Marel, G. A. van der; Ossendorp, F.; Codée, J. D. C. C.; van der Marel, G. A.; Ossendorp, F.; Codée, J. D. C. C. Multivalent, Stabilized Mannose-6-Phosphates for the Targeted Delivery of Toll-Like Receptor Ligands and Peptide Antigens. *ChemBioChem* **2021**, *22* (2), 434–440. https://doi.org/10.1002/CBIC.202000538.

(49) La–Venia, A.; Dzijak, R.; Rampmaier, R.; Vrabel, M. An Optimized Protocol for the Synthesis of Peptides Containing Trans-Cyclooctene and Bicyclononyne Dienophiles as Useful Multifunctional Bioorthogonal Probes. *Chem. – A Eur. J.* **2021**, *27* (54), 13632–13641. https://doi.org/https://doi.org/10.1002/chem.202102042.

(50) Boll, E.; Drobecq, H.; Ollivier, N.; Blanpain, A.; Raibaut, L.; Desmet, R.; Vicogne, J.; Melnyk, O. One-Pot Chemical Synthesis of Small Ubiquitin-like Modifier Protein–Peptide Conjugates Using Bis(2-Sulfanylethyl)Amido Peptide Latent Thioester Surrogates. *Nat. Protoc. 2014 102* **2015**, *10* (2), 269–292. https://doi.org/10.1038/nprot.2015.013.

(51) Zheng, J. S.; Tang, S.; Qi, Y. K.; Wang, Z. P.; Liu, L. Chemical Synthesis of Proteins Using Peptide Hydrazides as Thioester Surrogates. *Nat. Protoc. 2013 812* **2013**, *8* (12), 2483–2495.

https://doi.org/10.1038/nprot.2013.152.